

**Bond-slip Relationship of Carbon Fiber Reinforced Polymer (CFRP) Plated Steel  
Member under Fatigue Loading**

by

Azimah binti Mohd Hamdan

Dissertation submitted in partial fulfillment of  
the requirements for the  
Bachelor of Engineering (Hons)  
(Civil Engineering)

SEPT 2013

Universiti Teknologi PETRONAS  
Bandar Seri Iskandar  
31750 Tronoh  
Perak Darul Ridzuan  
Malaysia

CERTIFICATION OF APPROVAL

**Bond-slip Relationship of Carbon Fiber Reinforced Polymer (CFRP) Plated Steel  
Member under Fatigue Loading**

by

Azimah binti Mohd Hamdan

A project dissertation submitted to the  
Civil Engineering Programme  
Universiti Teknologi PETRONAS  
In partial fulfillment of the requirement for the  
Bachelor of Engineering (Hons)  
(Civil Engineering)

Approved by,

---

(Dr Ibrisam bin Akbar)

UNIVERSITI TEKNOLOGI PETRONAS  
TRONOH, PERAK  
September 2013

## ABSTRACT

This paper intended to discuss in depth the provision of the groundwork for the development of bond-slip relationship of carbon fiber reinforced polymer (CFRP) plated steel member under fatigue loading. The bond-slip characteristics of the adhesive joint between the CFRP and steel have been studied under monotonic load so that debonding does not occur whilst the members are in service. A typical bond-slip relationship is assumed to be bilinear consisting of an elastic branch which peaks at  $\tau_{\max}$  and the softening branch up to  $\delta_{\max}$ . However there are relatively few studies on the bond-slip relationship due to fatigue loading. Thus this research focuses to study the behavior of this composite system by thoroughly examining the shear stress distribution along the bonded length. Experimental program using single lap pull test subjected to monotonic loading is carried out using CFRP plated steel block. Later, fatigue life prediction of the composite system is done using stress-life approach in order to come up with a suitable fatigue loading program. The output of this research will be a firm base for a good formulation of the bond-slip relationship under fatigue loading and therefore will enhance the knowledge of time-dependant behavior for steel bridges, steel jetty and offshore platforms retrofitting as well as the development of design standard for fatigue conditions.

## **ACKNOWLEDGEMENT**

First and foremost, the author would like to praise Allah the Almighty for His guidance and blessing. Profound gratitude goes to Universiti Teknologi PETRONAS and Civil Engineering Department for the opportunity given to carry out this research.

Endless thanks and deep regards extended to the author's Supervisor, Dr Ibrisam bin Akbar for the exemplary guidance, monitoring and constant encouragement throughout the research accomplishment. The information, experiences sharing and assistance have helped to improve the author's knowledge and attitude towards accomplishing the research scope.

The author would also like to take immense pleasure to thank the fellow post-graduate students and laboratory technicians for the help and enthusiastic guidance. The author is enormously indebted for their cooperation and willingness in helping the author to explore and carrying out the research as intended.

Finally yet importantly, earnest thanks and love go to the author's parents, friends and family for their blessing supports and wishes for the successful completion of this research. Their presence and encouragement will always be a fond memory to the author.



## TABLE OF CONTENTS

TABLE OF CONTENTS .....	i
LIST OF FIGURES .....	iii
LIST OF TABLES .....	v
ABBREVIATIONS AND NOMENCLATURES .....	vi
CHAPTER 1: INTRODUCTION .....	1
1.1..... PROJECT BACKGROUND	1
1.2..... PROBLEM STATEMENT	2
1.3..... OBJECTIVES AND SCOPE OF STUDY	2
1.4..... RELEVANCY OF THE PROJECT	3
1.5..... FEASIBILITY OF THE PROJECT	3
CHAPTER 2: LITERATURE REVIEW .....	4
2.1..... FATIGUE	4
2.1.1 ..... Basic concept	4
2.1.2 ..... Stress cycles	5
2.1.3 ..... Forms of failure	7
2.1.4 ..... Process of fatigue failure	7
2.1.5 ..... S-N curve	9
2.2..... CARBON FIBRE REINFORCED POLYMER (CFRP)	11
2.3..... TEST METHODS	12
2.4..... PREVIOUS STUDIES ON FATIGUE	15
2.4.1 ..... Fatigue bond characteristic and behavior	15
2.4.2 ..... Fatigue life improvement	20
2.4.3 ..... Stiffness reduction due to fatigue loading	23
2.4.4 ..... Stress range effect	25
2.5..... EFFECTIVE BOND LENGTH	27
2.6..... MODES OF FAILURE	35
2.7..... BOND-SLIP RELATIONSHIP	36

2.8.....	CONCLUSION	38
CHAPTER 3: METHODOLOGY .....		39
3.1.....	RESEARCH METHODOLOGY	39
3.1.1 .....	Literature review	39
3.1.2 .....	Experimental program	39
3.1.3 .....	Data collection and analysis	47
3.2.....	PROJECT ACTIVITES	48
3.3.....	KEY MILESTONE AND GANTT CHART	49
3.4.....	TOOLS AND EQUIPMENTS	50
CHAPTER 4: RESULTS AND DISCUSSIONS.....		48
4.1	BEHAVIOUR OF CFRP PLATED STEEL MEMBER AND SHEAR STRESS DISTRIBUTION ALONG THE BONDED LENGTH .....	48
4.1.1 .....	Failure mode	48
4.1.2 .....	Bond-slip relationship	50
4.1.3 .....	Load-Displacement behavior	52
4.1.4 .....	Shear stress distribution along CFRP-Steel interface	52
4.2	FATIGUE LIFE PREDICTION USING STRESS-LIFE APPROACH ..	54
CHAPTER 5: CONCLUSION AND RECOMMENDATION .....		58
REFERENCES.....		60

## LIST OF FIGURES

Figure 2.1: Cyclic stresses .....	5
Figure 2.2: Alternating stress cycle.....	6
Figure 2.3: Tension/Tension loading .....	6
Figure 2.4: Random loading.....	6
Figure 2.5: Stages of fatigue crack .....	7
Figure 2.6: Development of extrusions and intrusions during fatigue .....	8
Figure 2.7: Crack propagation.....	8
Figure 2.8: SEM image of fatigue striations .....	9
Figure 2.9: Beach marks .....	9
Figure 2.10: Typical S-N curve .....	10
Figure 2.11: Comparison of steel and aluminum fatigue behavior .....	11
Figure 2.12: Bond testing methods .....	13
Figure 2.12: Bond testing methods (continued) .....	14
Figure 2.12: Bond testing methods (continued).....	15
Figure 2.13: Schematic diagram of 4-point bending test configuration .....	21
Figure 2.14: S-N plot of fatigue test data.....	22
Figure 2.15: Reduction in stiffness of retrofitted specimens during fatigue tests .....	24
Figure 2.16: Results of fatigue test (P-N curves).....	26
Figure 2.17: Experimental failure loads of all seven SLJ cases tested .....	28
Figure 2.18: Effective bond length for normal modulus CFRP joint .....	30
Figure 2.19: Effective bond length for CFRP joint .....	31
Figure 2.20: Effect of CFRP sheet layers number on effective bond length .....	32
Figure 2.21: Comparison of experimental and imperial model result .....	33
Figure 2.22: Schematic view of failure modes .....	35
Figure 2.23: Pull-off test set up .....	36
Figure 2.24: Bilinear bond-slip model .....	37
Figure 2.25: New proposed bond-slip model by Dehghani et al. (2012).....	38
Figure 3.1: Steel blocks after being sandblasted .....	40
Figure 3.2: Ball bearing glued to the steel surface .....	40
Figure 3.3: Sikadur 30 Part A and Part B .....	41



Figure 3.4: Mixing the adhesive .....	41
Figure 3.5: Placing weight on top of the CFRP plate .....	42
Figure 3.6: Installation of strain gauges along the CFRP plate .....	42
Figure 3.7: Single strap pull test specimen setup.....	43
Figure 3.8: Planned project activities.....	45
Figure 4.1: Debonding first occurred near the loaded end.....	48
Figure 4.2: Cohesive failure and cracks observed in the control specimen.....	49
Figure 4.3: Sample spreadsheet calculation to process the raw data.....	50
Figure 4.4: Bond-slip relationship for control specimen.....	51
Figure 4.5: Load-displacement curve.....	52
Figure 4.6: Shear stress distributions.....	53
Figure 4.7: Effect of using different $S_f$ coefficient on fatigue cycles .....	55
Figure 4.8: Effect of using different loading amplitude on number of cycles .....	56
Figure 4.9: S-N curve for the proposed experimental program .....	57

## LIST OF TABLES

Table 2.1: Material properties of adhesives. ....	16
Table 2.2: Specimen details and test results.....	16
Table 2.3: Material properties of adhesives. ....	17
Table 2.4: Bond strengths for cohesion failure. ....	17
Table 2.5: Material properties of adhesives. ....	18
Table 2.6: Test results. ....	18
Table 2.7: Test results of specimens survived fatigue loading. ....	19
Table 2.8: Test results for unretrofitted beams .....	20
Table 2.9: Test results for retrofitted beams .....	21
Table 2.10: Fatigue test results .....	23
Table 2.11: Specimen loading.....	24
Table 2.12: Beam details and test results .....	26
Table 2.13: Geometry and dimensions of the fabricated coupons.....	27
Table 2.14: Results of double strap joints.....	29
Table 2.15: Effective bond lengths of different CFRP-steel systems.....	29
Table 2.16: Results of specimen testing.....	30
Table 2.17: Test results .....	32
Table 2.18: Material properties .....	33
Table 2.19: Effective bond length specimen matrix and summary of test results ....	34
Table 3.1: Material properties .....	39
Table 3.2: Gantt Chart of the research project .....	46
Table 4.1: Fatigue loading program for CFRP plated steel member .....	57

## ABBREVIATIONS AND NOMENCLATURES

CFRP	Carbon Fiber Reinforced Polymer
UHM	Ultra High Modulus
$\sigma_{max}$	maximum stress
$\sigma_{min}$	minimum stress
$\sigma_m$ or $S_m$	mean stress
$\sigma_r$ or $\Delta\sigma$	stress range
$\sigma_a$ or $S_a$	stress amplitude
$S_{Nf}$	fatigue strength at failure
$S_f$	endurance limit
R	stress ratio
N	number of cycles
$f_{t,a}$ or $S_u$	ultimate tensile strength
$E_a$	Young's Modulus
$P_{ult}$	ultimate load
$G_f$	interfacial fracture energy
$F_{f,max}$	residual strength
$\beta$	degrees of fatigue damage
$t_a$	adhesive thickness
$t_p$	CFRP plate thickness
$w$	CFRP plate width
$\tau_s$	average shear stress
$\tau_f$	maximum shear stress
$l_{eff}$	effective bond length
$\delta$	displacement
$\delta_0$	maximum elastic displacement
$\delta_f$	displacement at failure



# CHAPTER 1

## INTRODUCTION

### 1.1 PROJECT BACKGROUND

Whether it is concrete, masonry or steel structures, all of them need proper maintenance in order to prolong the serviceability life. Many factors can be associated when it comes to structures aging and deterioration. Concerning steel structures, the factors include typical corrosion and fatigue.

One of the common approaches adopted to tackle fatigue issue is using steel plates either bolted or welded to the damaged steel structures. However, this approach is seemingly to be causing another problem due to the additional dead load imposed as well as the cost and time consideration. In addition, fatigue problem in welding connection makes both of these options not favorable.

A considerable interest has been given to the use of Fiber Reinforced Polymer (FRP) in strengthening existing structures including concrete and steel in recent years. FRP is a polymer matrix resin reinforced with fibers and has a lower modulus of elasticity compared to steel. The polymer can be epoxy, vinylester or phenol formaldehyde resins while glass, carbon, basalt or aramide make up the fibers component of FRP [1].

Some of the characteristics of the FRP that makes it preferred for structure strengthening including high strength, non-corrosive nature, light weight, fatigue resistant and linear elastic tensile stress-strain behavior. However, from recent studies, Carbon Fiber Reinforced Polymer (CFRP) is found to be the most suitable type for steel structures strengthening [2, 3]. Steel structures retrofitting using adhesively-bonded CFRP is one of the research areas that receive enormous attention in recent years.

It is proven from previous researches carried out that the bonding between the CFRP and steel members plays a vital role in ensuring successful forces transfer and hence causes lower stress concentrations. Most of the studies done before reported the failures to be likely occurring in the adhesive; hence it is very important to study the bond behavior between the CFRP and steel, especially under fatigue loading [3, 4].

## **1.2 PROBLEM STATEMENT**

Steel bridges, steel jetties and offshore platforms are the typical structures subjected to fatigue loading. The steel members used in the construction of these structures can experience millions of variable amplitude load cycles during their service life. Such fatigue loading represents a main cause of degradation in these structures. As a result, fatigue is an important consideration in their design criteria and should be given special attention. CFRP is identified as a potential remedy in steel structures retrofitting when subjected to such loading.

As observed throughout the years, in previous studies made by other researches, most of them solely focus on the bond characteristics between CFRP and steel when subjected to static tensile loading [2], pull-off test [4] and impact loading [5]. Less attention had been given to the effect of fatigue loading as well as the development of the bond-slip relationship in CFRP plated steel members subjected to such loading [6].

This report presents a systematic study to provide groundwork for the establishment of bond-slip relationship of CFRP plated steel member when it is subjected to fatigue loading. The groundwork hopefully will be useful for the formulation of the bond-slip relationship which is crucial for steel structures retrofitting particularly those subjected to fatigue loading; steel bridges, steel jetty and offshore platforms.

## **1.3 OBJECTIVES AND SCOPE OF STUDY**

With the fact that there is no established bond-slip relationship of CFRP plated steel member under fatigue loading, it is important to have solid and firm groundwork for the research project. The groundwork includes the identification of the composite system behavior as well as controlling parameters that might affect the fatigue study later.

Hence, the objectives of this paper are to:

1. establish the behavior and shear stress distribution along the bonded length of CFRP plated steel member; and
2. predict the fatigue behavior and fatigue life using stress-life approach.

A control specimen; adhesively bonded CFRP steel member will be first subjected to tensile loading until failure occurs. From this experiment, failure mechanisms and the behavior of the system will be thoroughly examined and analyzed in the form of graphs and discussions. From the data, the fatigue life of this composite system will be predicted using the stress life approach. All in all, this research will provide groundwork for the determination of the testing regime and later, the development of bond-slip relationship of CFRP plated steel member when subjected to fatigue loading.

#### **1.4 RELEVANCY OF THE PROJECT**

In view of the fact that less attention has been given to the bond-slip relationship analysis of CFRP plated steel member under fatigue loading, Zhao & Zhang [7] has suggested that researches on this area of study should be carried out to represent an initial step to fill the gap. Hence this research is important to provide groundwork for the formulation of the bond-slip relationship which will be a highly potential knowledge in the field of fatigue-damaged steel structures retrofitting.

#### **1.5 FEASIBILITY OF THE PROJECT**

Experimentally, the single strap pull test will be carried out using Universal Testing Machine (UTM) which is available at Universiti Teknologi PETRONAS Concrete Technology Laboratory located at Block 13. From the time frame point of view, within eight months of the Final Year Project I and II courses, the planned scope of study is hopefully manage to be achieved.





## **CHAPTER 2**

### **LITERATURE REVIEW**

Issues and topics concerning fatigue concept, CFRP-to-steel bond behavior and bond-slip relationship will be discussed accordingly in each section. Findings from several related journals, proceedings, books, and reports reviewed by the author are presented in this chapter.

#### **2.1 FATIGUE**

##### **2.1.1 Basic concept**

Fatigue concept in simple language, is when a motion is repeated, the object that is doing the work becomes weak and eventually fails at a stress level below the nominal strength of the material. It is the progressive, localized and permanent structural change that may occur in materials or structures when subjected to repeated stresses over a long period of time. When this occurs, it can lead to cracks and later cause fracture after sufficient fluctuations are achieved [8].

Failure by fatigue is a fairly common occurrence, as many components are subjected to alternating or fluctuating loads during their service life. Fatigue has been estimated to be the prominent cause of all mechanical service failures [9] and structural degradation of existing bridges and infrastructures in Europe, North America and Japan [6].

Campbell [9] discusses the three fundamental factors that must exist concurrently in order to cause fatigue:

1. maximum tensile stress of sufficiently high value;
2. sufficient fluctuation of applied stress; and
3. sufficient large number of cycles of the applied stress.

However, different approach was adapted by Boardman [8] to explain the necessary simultaneous action needed to cause fatigue namely cyclic stress, tensile stress and plastic strain. Without these three components, fatigue crack will not initiate and propagate due to the fact that the plastic strain caused by the cyclic stress will initiate the cracks and the propagation of the cracks is induced by the tensile stress.

### 2.1.2 Stress cycles

In order to cause fatigue, there are many types of fluctuating stresses that can be applied. A typical stress cycle is characterized by maximum ( $\sigma_{max}$ ), minimum ( $\sigma_{min}$ ) and mean stress ( $\sigma_m$ ), range of stress ( $\sigma_r$ ), the stress amplitude ( $\sigma_a$ ) and the stress ratio  $R = \sigma_{min}/\sigma_{max}$  as shown in Figure 2.1.

$$\sigma_r = \sigma_{max} - \sigma_{min}$$

$$\sigma_a = \frac{\sigma_{max} - \sigma_{min}}{2}$$

$$\sigma_m = \frac{\sigma_{max} + \sigma_{min}}{2}$$

According to Kelly [10], the simplest is the fully reversed stress cycle or alternating as shown in Figure 2.2 which is commonly used in testing. Figure 2.2 shows a sine wave where the negative sign differentiate the maximum and minimum stress applied. In this condition, the mean stress which is the algebraic average of the maximum stress and minimum stress in once cycle is equal to zero [8]. The simplest example where this type of stress cycle occurs is in an axle; at every half turn or half period as in the case of the sine wave, the stress on a point would be reversed.

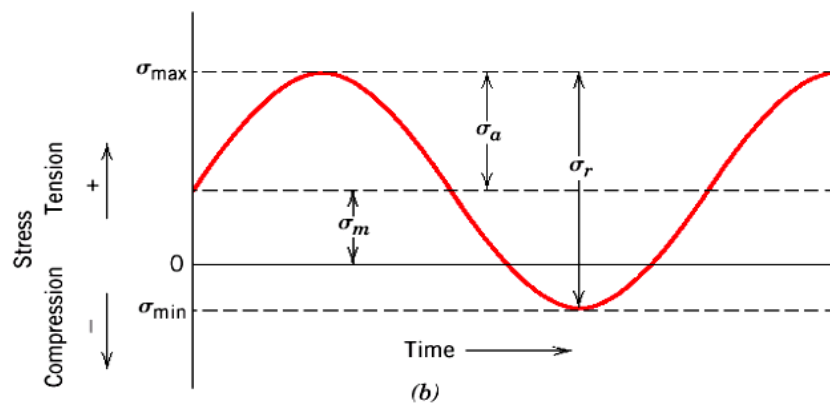


Figure 2.1: Cyclic stresses.

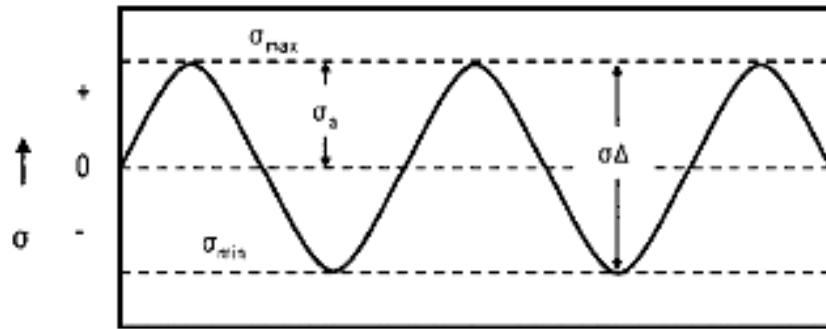


Figure 2.2: Alternating stress cycle. [9]

Figure 2.3 on the other hand shows the condition of pulsating tensile stress in which both the cyclic and applied stresses are positive stresses, but it is also possible to have stresses in compression; negative stresses. This type of stress cycle is also called repeated stress cycle [10].

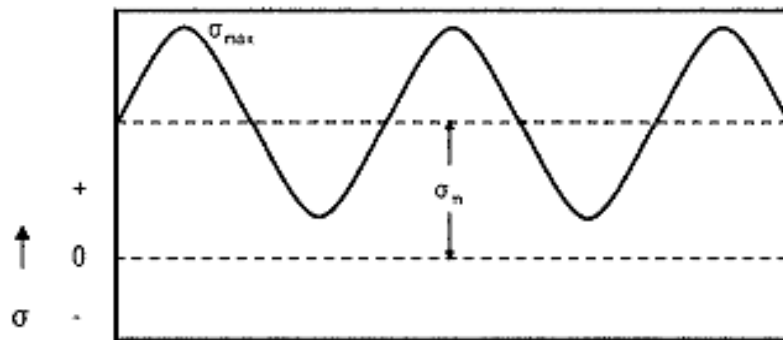


Figure 2.3: Tension/Tension loading. [9]

The final type of stress cycle will be the random or irregular stress cycle, in which the stress and frequency vary randomly as shown in Figure 2.4.

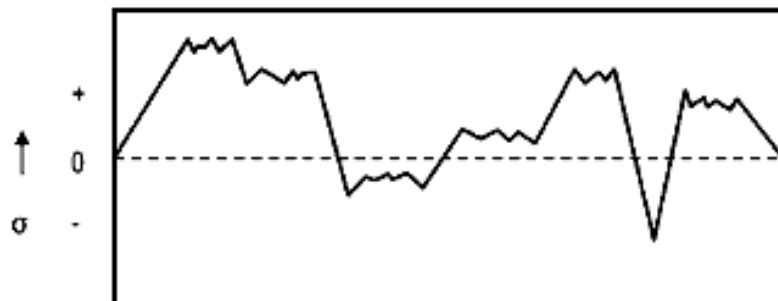


Figure 2.4: Random loading. [9]

According to Jackson & Dhir [11], much fatigue testing is carried out using alternating stress cycles and the results of many tests are expressed in the form of an S-N plot, where S is the maximum stress in a cycle and N is the number of cycles to failure. Further discussion on the S-N curve is clarified in Section 2.1.5.

### 2.1.3 Forms of failure

Failure by fatigue takes two forms; low-cycle fatigue and high-cycle fatigue [9, 11]. The former type is when the maximum stress in any cycle is larger than the yield stress, although less than the static tensile strength and failure occur at a low number of cycles, generally less than 1000. The latter type obviously is the contradiction of the former where the maximum stress is lesser than the yield stress and  $10^5$  to  $10^6$  cycles may be required to cause the failure. Plastic and elastic deformation takes place in low-cycle fatigue while only elastic deformation occurs in high-cycle fatigue.

### 2.1.4 Process of fatigue failure

In general, there are three stages of fatigue fracture process as shown in Figure 2.5 [8, 9, and 12]:

1. crack initiation;
2. crack propagation or growth; and
3. ultimate failure (fracture).

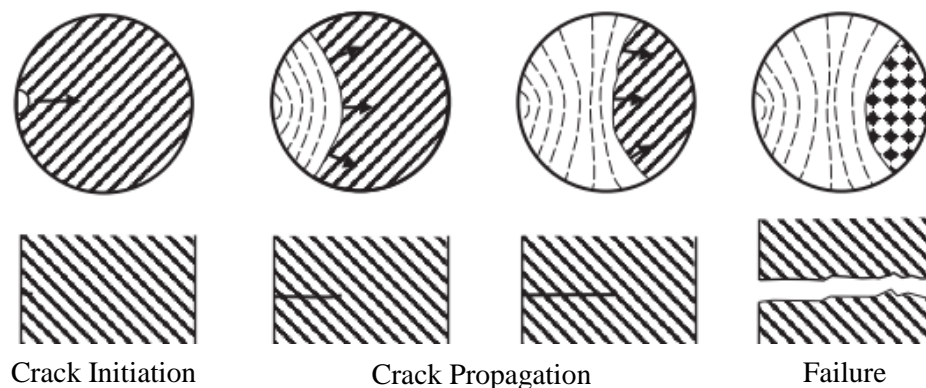


Figure 2.5: Stages of fatigue crack. [9]

Campbell [9] proposed that the crack initiation often starts at a notch or surface irregularity. However, this is not true all the time such that crack initiation will eventually occur due to the formation of persistent slip bands (PSBs) even with the absence of surface defects. PSBs are formed when dislocations accumulate near

surface stress concentrations and can be either extrusion (rise above) or intrusion (fall below) as shown in Figure 2.6. Continuous back-and-forth movement of these band slips will eventually cause the cracks formation.

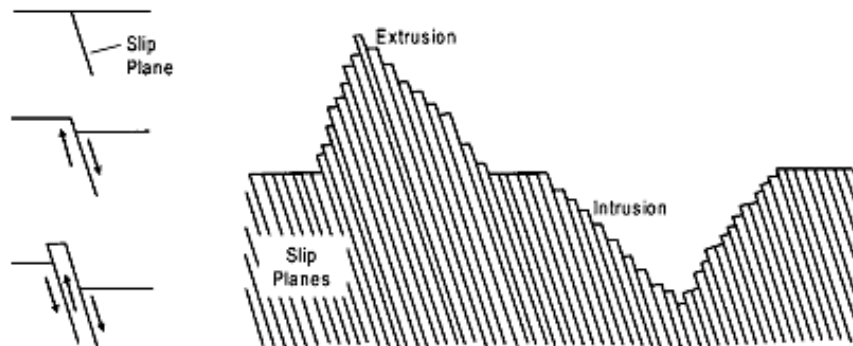


Figure 2.6: Development of extrusions and intrusions during fatigue. [9]

When enough crack length is achieved, the stress field at the tip becomes dominant and will change the overall crack plane to the direction normal to the principal stress and the crack enters the next stage; crack propagation or growth.

During crack growth, continuous crack sharpening takes place proceeds by blunting as illustrated in Figure 2.7. A pattern of crack striations are produced during the crack growth and each of these striations corresponds to one fatigue cycle as shown in Figure 2.8. Nevertheless, fatigue failure can still occur without the formation of these striations which can only be identified using scanning electron microscope (SEM). Through visual examination, beach marks are easier to be identified as shown in Figure 2.9.

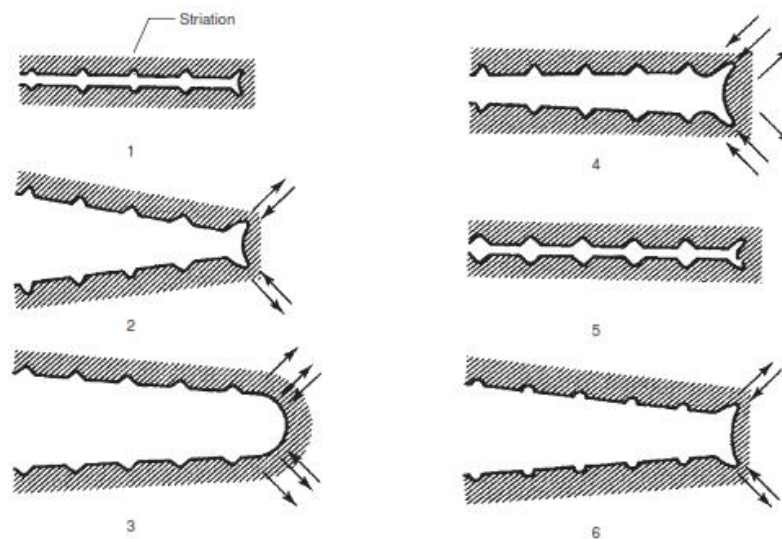


Figure 2.7: Crack propagation. [9]

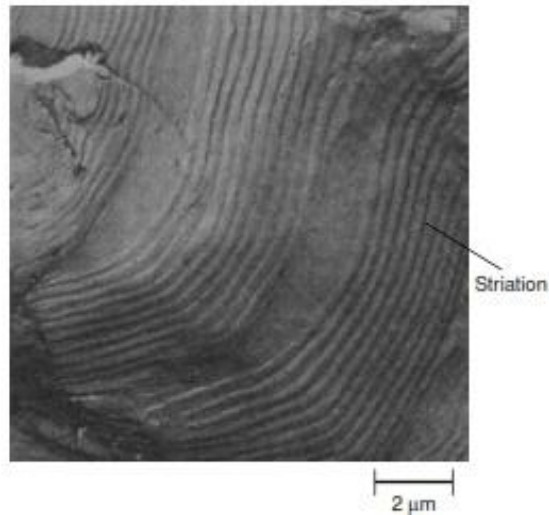


Figure 2.8: SEM image of fatigue striations. [9]

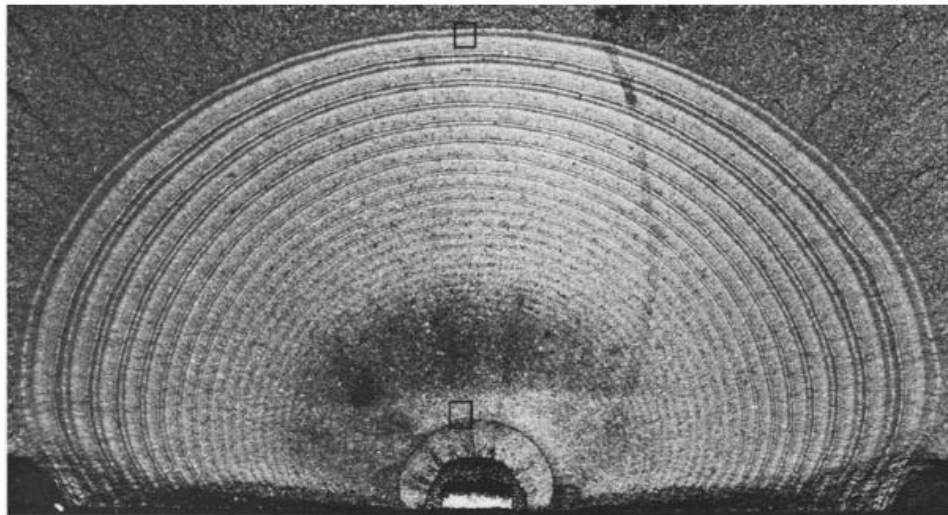


Figure 2.9: Beach marks. [9]

The next stage is when the cracks are long enough and the material or structure could no longer support the applied load, ultimate fatigue failure will occur.

### 2.1.5 S-N curve

An S-N curve is used to characterize the material performance subjected to fatigue loading and usually adopted in presenting high-cycle fatigue data [9]. For the designer, it is critical that this relationship be characterized so that fatigue life can be predicted. It is a plot of the stress,  $S$ , which can be the maximum stress ( $\sigma_{\max}$ ), minimum stress ( $\sigma_{\min}$ ) or the stress amplitude ( $\sigma_a$ ) versus  $N$ , the number of cycles to failure. Most often the values of  $N$  are plotted on a logarithmic scale since they are generally quite large. Typical S-N curve is shown in Figure 2.10.

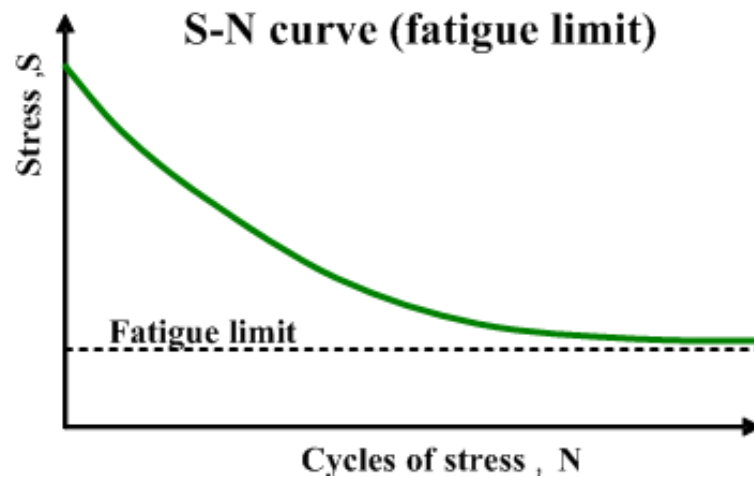


Figure 2.10: Typical S-N curve.

It is important to identify the characterization of the S-N curve in fatigue analysis study. Plotting the S-N curve is based on the fatigue life, which is the number of cycles required to cause failure at specified stress level. The fatigue life reduces with respect to the increase in applied stress and at a limiting value of stress, the curve flattens off and it is identified as the endurance limit or fatigue limit for the specific material [12]. Under this limit, the applied stress will not induce any failure. For any structural design, the members should be designed to resist fatigue by ensuring that the stress in the member does not exceed its endurance limit [13].

Both Campbell [9] and Hibbeler [13] demonstrate the apparent comparison of the fatigue behavior in steel and aluminum as shown in Figure 2.11. Steel not only have higher fatigue strength than aluminum, but it also have endurance limit. Aluminum will always fail if tested to a sufficient number of cycles and hence it is normally specified as the stress having a limit of 500 million cycles. Typical values of endurance limits for various engineering materials are usually reported in handbooks.

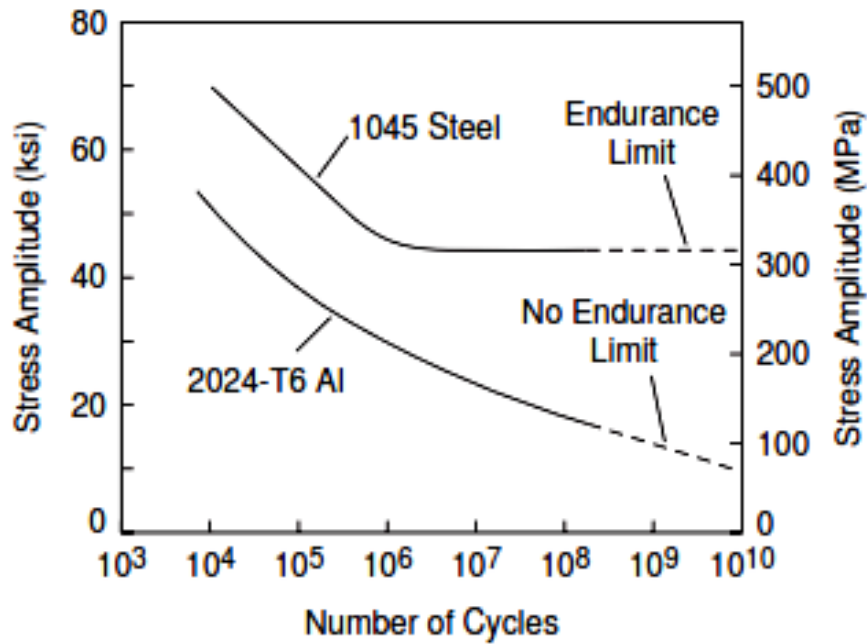


Figure 2.11: Comparison of steel and aluminum fatigue behavior. [9]

## 2.2 CARBON FIBRE REINFORCED POLYMER (CFRP)

Fiber reinforced polymer (FRP) is a polymer matrix resin reinforced with fibers and has a lower modulus of elasticity compared to steel. There is nowadays a wide range of available types of FRP composites (with polyester, epoxy or vinyl-ester matrices) reinforced with glass, carbon and aramid fibers with suitable properties for different applications in civil and structural engineering [14].

Besides the distinctive features of FRP (light weight, high strength, non-corrosive and high resistance to fatigue) that make it preferred for structures strengthening, Nicolae et al. [14] have also identified some drawbacks of using FRP in structures reinforcement:

1. FRP composites are typically brittle materials.
2. Ultimate tensile strength of FRP reinforcing bars decreases with the bar diameter.
3. The compressive behavior of FRP bars has not been studied adequately and a tendency to buckle sooner than the steel bars has been noticed.
4. Entrapped air due to uncontrollable adhesive layer quality can affect the bond between FRP and the bonded structures.



Despite the reported disadvantages of using FRP in structures, recent researches findings are seemingly to come into a consensus that the use of FRP specifically carbon FRP (CFRP) is beneficial to steel structures retrofitting after subjected to fatigue loading. These structures include bridges, towers, and platforms.

In the last decade, CFRP composite materials have been increasingly employed in the construction industry, mainly in applications dealing with structural strengthening and repair. They are ideally suited for this purpose, due to a combination of the very high stiffness-to-weight and strength-to-weight ratios and an excellent durability in aggressive environments.

Apart from reported studies on the effectiveness of CFRP in concrete structures strengthening [15], advance CFRP composites have been proposed as excellent reinforcement materials for the fatigue strengthening of steel structures [4, 7, 16, 17].

CFRP plates on cracked steel sections may produce retardation or complete stop of the crack propagation by acting in three ways [18]:

1. reducing crack opening displacement at and behind crack front and therefore reducing stress intensity factors at the crack tip;
2. producing crack closure effect; and
3. increasing the stiffness of the cracked steel sections.

### **2.3 TEST METHODS**

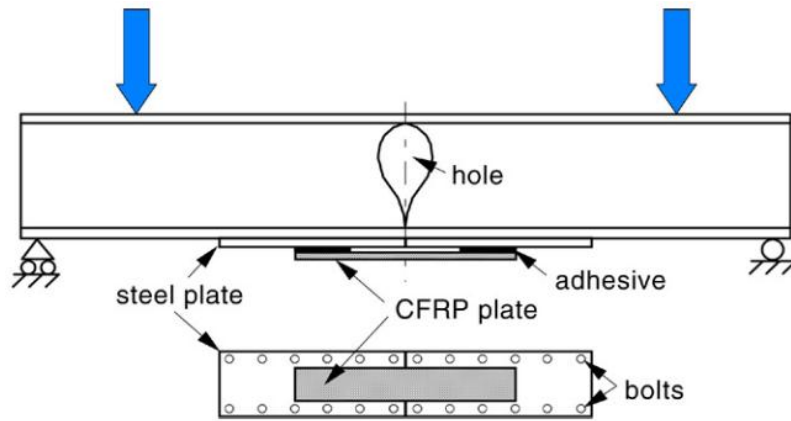
As discussed by Zhao & Zhang [7], different testing methods were adopted by various researches to test the bond for different purposes of study. Namely there are four types:

Type 1: The loading is indirectly applied to the FRP and steel plate in a beam (see Figure 2.12 (a));

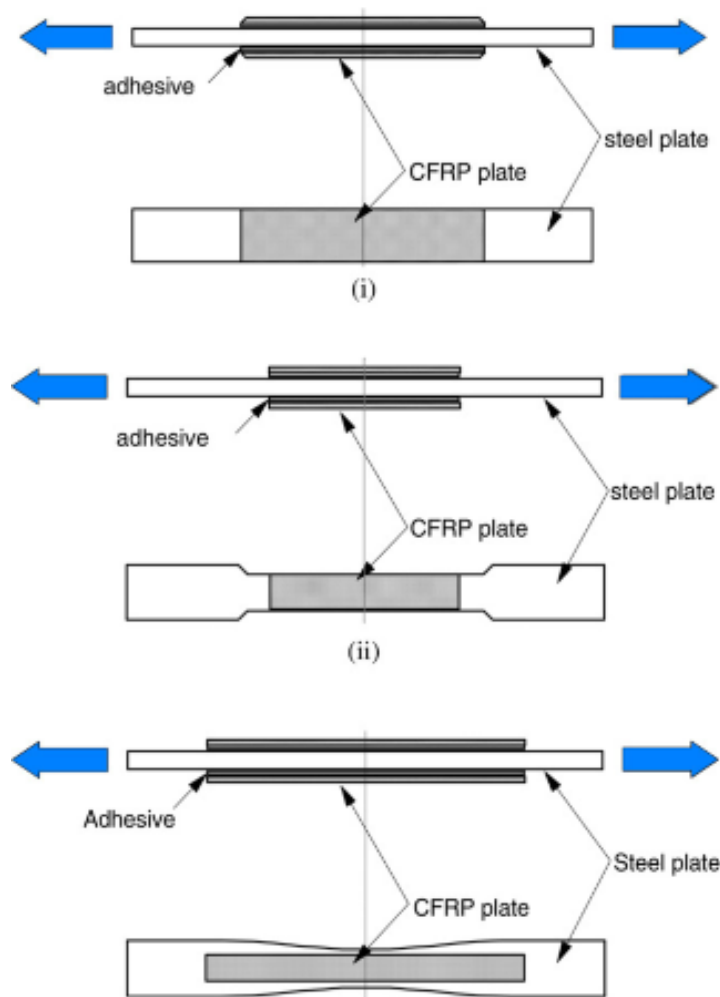
Type 2: The loading is directly applied to the steel element without any gap (see Figure 2.12 (b));

Type 3: The loading is directly applied to the steel element with a gap (see Figure 2.12 (c)); and

Type 4: The loading is directly applied to the CFRP (see Figure 2.12 (d)).



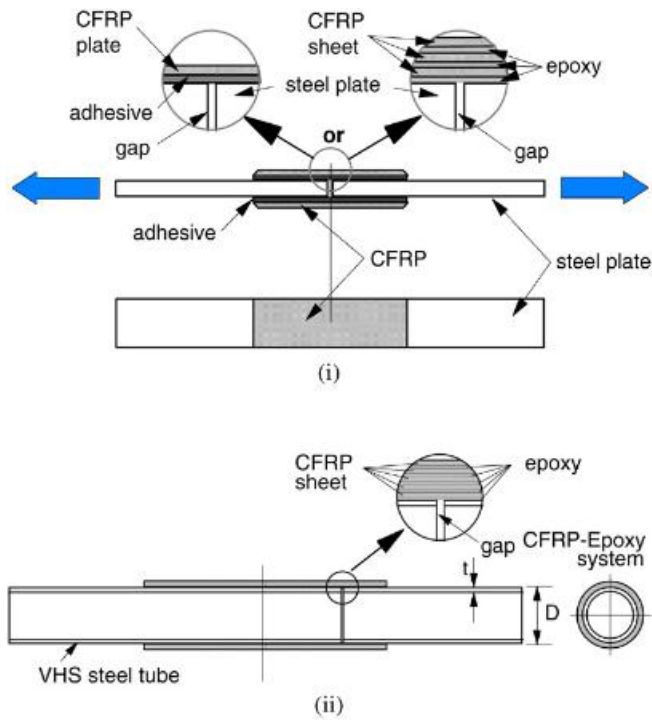
(a) Type 1: Loading is indirectly applied to the FRP and steel plate in a beam [19].



(b) Type 2: Loading is directly applied to the steel element without any gap.

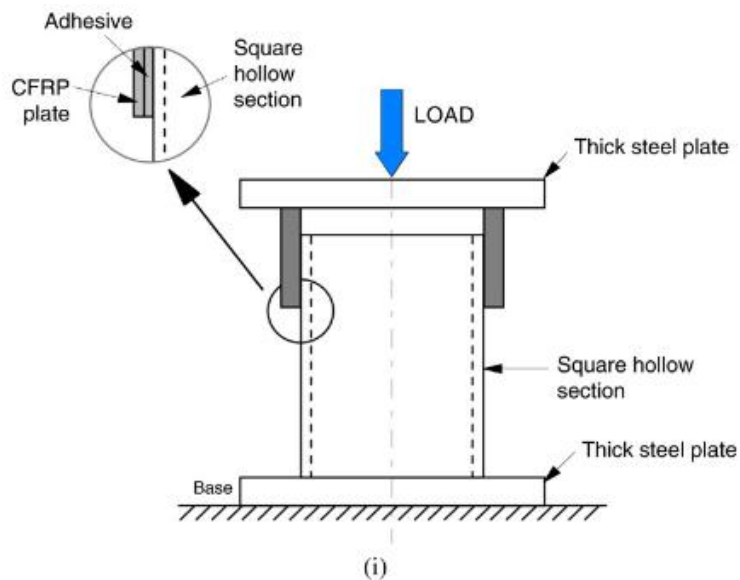
(i) Uniform width [1] (ii) Coupon shape [20] (iii) Dogbone shape [21]

Figure 2.12: Bond testing methods.



(c) Type 3: Loading is directly applied to the steel element with a gap.

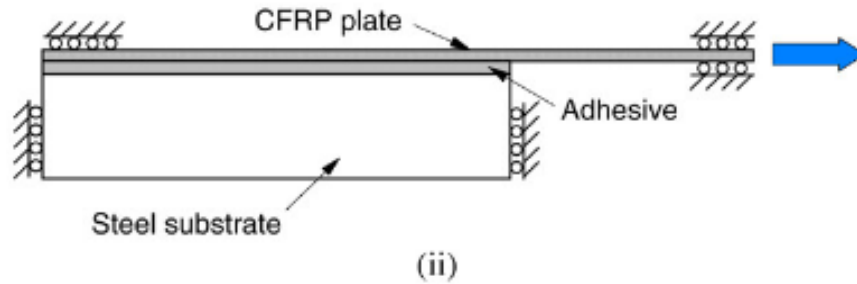
(i) Double strap joints [20, 22, 23] (ii) Single lap joint with circular hollow section [24, 25]



(d) Type 4: Loading is directly applied to the CFRP.

(i) Shear lap tests [26].

Figure 2.12: Bond testing methods (*continued*)



(d) Type 4: Loading is directly applied to the CFRP.

(ii) Single lap shear joint [4].

Figure 2.12: Bond testing methods (*continued*)

Each of the methods are designed for different testing objective and Zhao & Zhang [2] recommended to use the test set up shown in Figure 2.12 (d)(ii) to establish the bond-slip relationship between CFRP and steel in tension.

## 2.4 PREVIOUS STUDIES ON FATIGUE

### 2.4.1 Fatigue bond characteristic and behavior

While extensive research has been done to study the effectiveness of CFRP strengthened steel members, only recently research works had been performed to investigate the effects of fatigue loading on the CFRP plated steel members when different parameter are varied. The CFRP is commonly bonded to the existing structures with the use of adhesive such as epoxy. Based on previous studies, it has been identified that the critical difference between CFRP-to-concrete and CFRP-to-steel bonded interfaces is that concrete being the weak link in the former but in the latter, the weak link is the adhesive [3, 4].

When it comes to CFRP-strengthened steel, typical modes of failure are either the CFRP rupture or debonding of the FRP laminate along the CFRP-to-steel interface [4]. Hence it is very important to first understand the bond behavior of the CFRP-to-steel bonded interfaces before going deeper into the effects of different loading applied on the bond.

There are several controlling factors that may affect the bond behavior of the adhesively bonded CFRP-to-steel. Xia & Teng [4] conducted a single pull-off experiment to investigate the effects of adhesive properties and adhesive thickness on bond behavior. Three types of adhesive with different tensile strength were used with properties shown in Table 2.1 and the thickness of the adhesive layer was varied to achieve a wide range of values of the adhesive stiffness. From the study, it can be deduced that practical adhesive thickness (<2mm) will cause adhesive failure while thickness greater than that will lead to debonding by plate delamination. The test results are as shown in Table 2.2.

Table 2.1: Material properties of adhesives [4]

<b>Adhesive</b>	<b>Tensile strength <math>f_{t,a}</math> (MPa)</b>	<b>Young's Modulus <math>E_a</math> (MPa)</b>
<b>A</b>	22.53	4013
<b>B</b>	20.48	10793
<b>C</b>	13.89	5426

Table 2.2: Specimen details and test results [4]

<b>Specimen</b>	<b>Intended/ measured adhesive thickness (mm)</b>	<b>Ultimate Load <math>P_{ult}</math> (kN)</b>	<b>Debonding failure mode</b>
<b>A-1</b>	1/1.07	60.5	Adhesive
<b>A-2a</b>	2/1.98	61.7	Adhesive
<b>A-2b</b>	2/1.84	55.6	Delamination
<b>A-4</b>	4/3.88	50.7	Delamination
<b>A-6</b>	6/6.12	53.2	Delamination
<b>B-1</b>	1/0.825	39.4	Adhesive
<b>B-2a</b>	2/1.90	42.4	Adhesive
<b>B-2b</b>	2/1.76	38.8	Adhesive
<b>B-4</b>	4/3.98	47.5	Adhesive /Delamination
<b>B-6</b>	6/6/05	55.9	Delamination
<b>C-1</b>	1/0.875	38.0	Adhesive /Delamination
<b>C-2a</b>	2/1.58	46.8	Adhesive /Delamination
<b>C-2b</b>	2/1.82	46.4	Adhesive /Delamination

Yu et al. [3] presented an experimental study on the CFRP-to-steel bonded interfaces behavior where several variables were considered including the material properties, adhesive thickness and the axial rigidity of the CFRP plate. The study demonstrated that the bond strength which is the ultimate tensile force that can be resisted by the CFRP plate before debonding depends strongly on the interfacial fracture energy; the area under the bond-slip curve as shown in Table 2.4. Apart from that, there exists the practical thickness of the adhesive with range of 1-2 mm. Thicker adhesive layer appears to increase the bond strength of the joint but further researches is needed to thoroughly clarify the effect.

Table 2.3: Material properties of adhesives [3]

Adhesive	Tensile strength	Young's Modulus
	$\sigma_{max}$ (MPa)	$E_a$ (GPa)
<b>A (Sika 30)</b>	22.34	11.25
<b>B (Sika 330)</b>	31.28	4.82
<b>C (Araldite 2015)</b>	14.73	1.75
<b>D (Araldite 420)</b>	21.46	1.83

Table 2.4: Bond strengths for cohesion failure [3]

Series	Specimen	Adhesive thickness (mm)	Interfacial Fracture Energy, $G_f$ (N/mm)	Bond Strength, $P_{ult}$ (kN)
<b>I</b>	A-NM-T1-I	1.07	1.06	30.75
	A-NM-T1-II	1.03	1.11	31.21
	C-NM-T1-I	0.99	12.34	112.87
	C-NM-T1-II	1.02	12.78	113.81
<b>II</b>	A-NM-T1.5	1.53	1.27	35.20
	A-NM-T2	2.06	1.54	40.00
	A-NM-T3	3.04	1.11	33.80
<b>III</b>	A-MM-T1	1.01	1.06	46.90
	A-HM-T1	1.20	1.31	63.80
	C-MM-T1	1.04	12.52	130.50

Different approach was used by Wu et al. [2] where they carried out experiment to study the bond characteristic of the CFRP-to-steel joints using two different types of adhesives and CFRP elastic modulus. Thirteen double straps joints as shown in Table 2.6, the failure modes and bond strengths were dependent on the adhesive properties whose properties are tabulated in Table 2.5. CFRP rupture or delamination was observed taken place in specimens using the Araldite 420 which apparently have higher tensile strength. While for specimens using Sikadur 30, cohesive failure occurred. This is due to the fact that this adhesive has much lower tensile strength.

Table 2.5: Material properties of adhesives [2]

<b>Adhesive</b>	<b>Tensile strength</b> $\sigma_{max}$ (MPa)	<b>Young's Modulus</b> $E_a$ (MPa)
<b>Araldite 420</b>	28.6	1901
<b>Sikadur 30</b>	24.0	9282

Table 2.6: Test results [2]

<b>Specimen</b>	<b>Adhesive Thickness</b>	<b>Bond Strength, <math>P_{ult}</math></b> (kN)	<b>Failure Mode</b>
<b>A260</b>	0.39	274.95	CFRP rupture
<b>A250</b>	0.38	267.34	CFRP rupture
<b>A120</b>	0.36	271.18	CFRP delamination
<b>A100</b>	0.31	250.63	CFRP delamination
<b>A70</b>	0.34	178.88	CFRP delamination
<b>A50</b>	0.36	137.23	CFRP delamination
<b>A30</b>	0.35	72.97	CFRP delamination
<b>S250</b>	0.43	151.33	Cohesive failure
<b>S100</b>	0.40	148.42	CFRP delamination and cohesive failure
<b>S80</b>	0.35	158.07	Cohesive failure
<b>S70</b>	0.40	126.44	Cohesive failure
<b>S50</b>	0.43	136.35	Cohesive failure
<b>S30</b>	0.34	58.51	Cohesive failure

In different experiment, Wu et al. [27] carried out a series of static and fatigue tests using double strap joints of UHM CFRP plates and steel plate to study the effect on bond strength. Five specimens were tensioned to failure under static loading of 90 kN as control specimens while the other twelve specimens were tested under fatigue loading with load ratios ranging from 0.2 to 0.6. From this study, a clearer comparison and investigation were made with respect to the control specimen regarding the effect of fatigue loading. The test results for those specimens that survived fatigue loading and subsequently subjected under static loading are tabulated in Table 2.7. It appeared that the residual bond strength decreased when higher fatigue load ratio is applied. However, the maximum reduction in the residual bond strength was only 4.27%, indicating that the fatigue load ratio had a very limited effect on the bond strength.

Table 2.7: Test results of specimens survived fatigue loading. [27]

<b>Specimen</b>	<b>Fatigue load range <math>\Delta P</math> (kN)</b>	<b>Load ratio <math>P_{max}/F_{s,max}</math></b>	<b>Residue strength <math>F_{f,max}</math> (kN)</b>
<b>A260</b>	0.39	274.95	165.35
<b>A250</b>	0.38	267.34	147.42
<b>A120</b>	0.36	271.18	152.62
<b>A100</b>	0.31	250.63	149.56
<b>A70</b>	0.34	178.88	141.76
<b>A50</b>	0.36	137.23	139.01
<b>A30</b>	0.35	72.97	138.43

However, since the study is performed using UHM CFRP plates, little fatigue effect can be observed using visual inspection and hence microscopic investigation is used to explain the effect of fatigue loading on residual bond strength.

Liu, Zhao, & Al-Mahaidi [28] on the other hand carried out a series of fatigue test with the use of both normal modulus and HM CFRP. Different level of constant amplitude stress ranges were adopted for the fatigue loading testing. The specimens were eventually tested in tension and the effect of fatigue loading on the failure modes, bond slip and bond strength was observed. It is found that the applied fatigue loading plays a vital role; when the maximum applied load is less than 40% of the ultimate static strength there was no fatigue failure in the specimens; and no



significant influence on the bond strength when the maximum applied load is less than 35% of the ultimate static strength. Also, it was concluded that normal modulus CFRP bonded specimens are more sensitive to fatigue cycles, whereas high modulus CFRP bonded specimens are more sensitive to the applied load ranges.

#### 2.4.2 Fatigue life improvement

Apart from that, CFRP patches were also proven to be able to extend the fatigue lifetime of the material [29, 30]. However, it is important to note the influence of some parameters on the effectiveness of this method such as the CFRP stiffness, adhesive thickness and size of debonded region [18].

Tavakkolizadeh & Saadatmanesh [30] carried out a series of tests to study the fatigue life improvement of damaged steel girders when repaired with pultruded carbon fiber sheets. Different stress ranges of 69 to 379 MPa were considered in the study using four-point bending test. In order to establish a reliable set of control data, seven pairs of unretrofitted beams were subjected to constant stress range cycles of 138, 172, 207, 241, 276, 310 and 345 MPa. As for the retrofitted specimens, a total of six retrofitted beams were subjected to constant stress range cycles of 207, 241, 276, 310, 345, and 379 MPa.

Table 2.8: Test results for unretrofitted beams. [30]

Stress Range (MPa)	Number of Cycles	
	Crack Initiation	Failure
207	69,760	119,140
241	32,495	71,278
276	14,511	35,710
310	10,019	30,216
345	7,606	19,068

From Table 2.9, it can be seen clearly that the use of CFRP sheet can prolong the fatigue life of damaged specimens. Retrofitted specimens experienced longer fatigue lives of between 2.6 to 3.4 times the unretrofitted specimens for stress ranges of 345 to 207 MPa, respectively. This improvement is equivalent to upgrading the detail from the AASHTO category D to category C.

Table 2.9: Test results for retrofitted beams. [30]

Stress Range (MPa)	Number of Cycles	
	Crack Initiation	Failure
207	152,414	379,824
241	92,687	241,965
276	35,966	105,345
310	21,655	75,910
345	16,786	54,300
379	7,146	35,356

Schnerch et al. [31] demonstrated the increment in ultimate strength of the strengthened bridge girders as well as a better fatigue performance when the beam is strengthened with CFRP if compared to conventional steel details in steel highway bridge construction. In their experiment, two different reinforcing systems were adopted where strengthened specimen is compared to the unstrengthened ones. The result showed an increment in allowable live load when the strengthened specimens were tested with a 20% increment of the applied load range.

A comparative study was carried out by Jiao, Mashiri & Zhao [32] where three methods of damaged steel beam retrofitting were used; welding, welding and bonding with CFRP plates or CFRP woven sheets laminated via a wet lay-up process. A 4 point bending test upon a beam that has initial cut was carried out for the purpose of this study as shown in Figure 2.13.

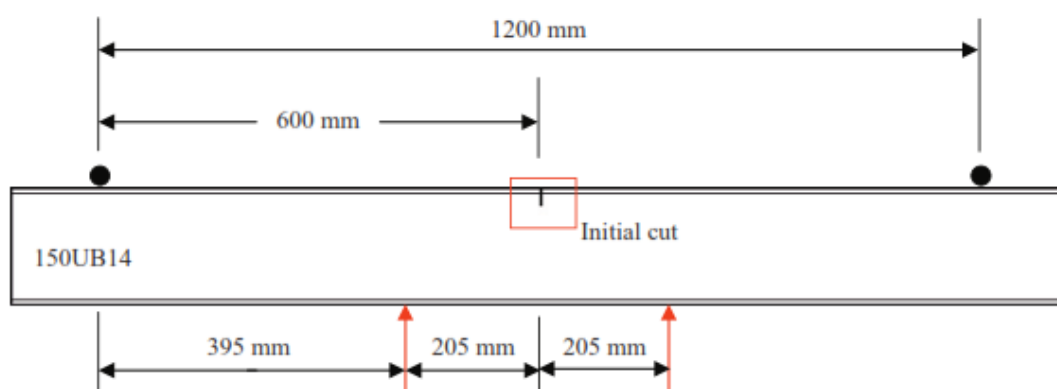


Figure 2.13: Schematic diagram of 4-point bending test configuration. [32]

From the study, it was found that one layer of CFRP plates can extend the fatigue life about 7 times compared to the beam retrofitted with solely welding method. 4 layers of CFRP woven sheets on the other hand can extend the fatigue life up to 3 times. This proved that beam strengthened with CFRP plates have better performance than those retrofitted with CFRP woven sheets. Mean S-N curves were obtained and can be used to predict the fatigue life of steel beams retrofitted with similar CFRP materials as shown in Figure 2.14. However, they reported that no significant difference in fatigue life could be observed when different adhesive were used.

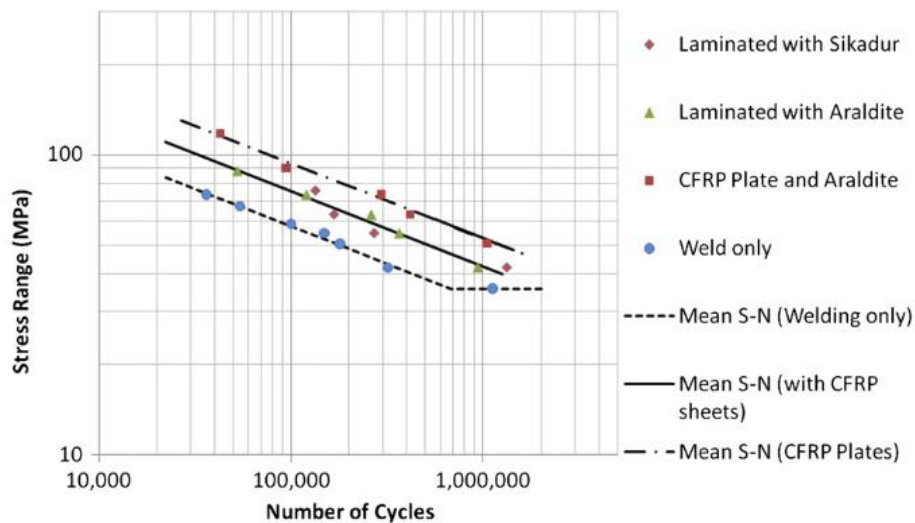


Figure 2.14: S-N plot of fatigue test data. [32]

As suggested by Jiao, Mashiri & Zhao [32], there is a need to study the influence of damage degree to the efficiency of using CFRP strengthening system. Hence, Yu et al. [33] performed an experimental and analytical study to deliver this need. In the series of tests, different lengths of artificial cracks were used to represent different degrees of fatigue damage, defined by  $\beta$ , which are 2%, 10% and 20% corresponding to initial crack length of 1mm, 5mm and 10mm. The technique of “beach marking” was adopted to trace the crack propagation and was proven to be a reliable method of recording crack shapes during fatigue testing for later measurement as concluded by Liu, Zhao, & Al-Mahaidi [28]. From the study, it was found that all the strengthened specimens had their fatigue lives prolonged by 97% to 186% compared to the unstrengthened specimens as tabulated in Table 2.10. A more significant extension of fatigue life was observed at a large damage level with late strengthening. However, early repair is suggested.

Table 2.10: Fatigue test results [33]

<b>Specimen</b>	<b>Number of fatigue cycles</b>	<b>Improvement (%)</b>
Unstrengthened specimen with a damage degree of 2%	234533	-
Strengthened specimen with a damage degree of 2%	462679	97%
Unstrengthened specimen with a damage degree of 10%	123738	-
Strengthened specimen with a damage degree of 10%	234710	90%
Unstrengthened specimen with a damage degree of 20%	65625	-
Strengthened specimen with a damage degree of 20%	187856	186%

Liu, Zhao, & Al-Mahaidi [28] carried out a series of experiments to investigate the effectiveness of CFRP on preventing fatigue crack propagation and extending the fatigue life of steel plates. Using single-sided and double-sided repairs with normal modulus or high modulus CFRP, the results showed that the application of the CFRP significantly reduced crack growth and extended the fatigue life. However, high modulus CFRP was found to be much more efficient when it can prolong the fatigue life up to 4.7-7.9 times while the normal modulus CFRP can only extend up to 2.2-2.7 times. Besides, they also varied the parameters of patch thickness, patch length and patch configuration to further study the governing factors. While the patch thickness and patch length influenced fatigue life of over 20% increment, patch configuration had only 6% influence on fatigue life increment.

### **2.4.3 Stiffness reduction due to fatigue loading**

In a series of fatigue tests conducted by Matta et al [34], a double sided reinforcement and double-sided shear lap joints were subjected to fatigue loading. The results showed that the member stiffness gradually decreased throughout the fatigue loading. Liu, Zhao, & Al-Mahaidi [28] on the other hand carried out a series of fatigue test with the use of both normal modulus and HM CFRP. Different level of constant amplitude stress range was adopted for the fatigue loading testing. The specimens were eventually tested in tension. A good agreement on a reduction on bond slip stiffness was found due to the damage accumulated during the fatigue

loading. However, the reduction in bond strength is not significant as it was only about 7%.

Bocciarelli et al. [6] performed preliminary tests at different loading conditions under constant stress range cycles of 83, 100, 120 and 160 MPa. From the tests, significant stiffness reduction is observed due to progressive debonding of the adhesive as shown in Figure 2.15. During the crack initiation, the stiffness reduced to 98% and reached 95% stiffness reduction when the delamination started to advance rapidly. When the CFRP debonding reached the midspan of the specimens, the stiffness dropped to 85% of the original value. From the experiments, it is concluded that fatigue performance could be improved by optimizing the joint design other than selecting suitable CFRP plate thickness and elastic modulus as well as adhesive thickness.

Table 2.11: Specimen loading [6]

Specimen	$\Delta\sigma$ (MPa)
FT1	83
FT2	100
FT3	120
FT4	160

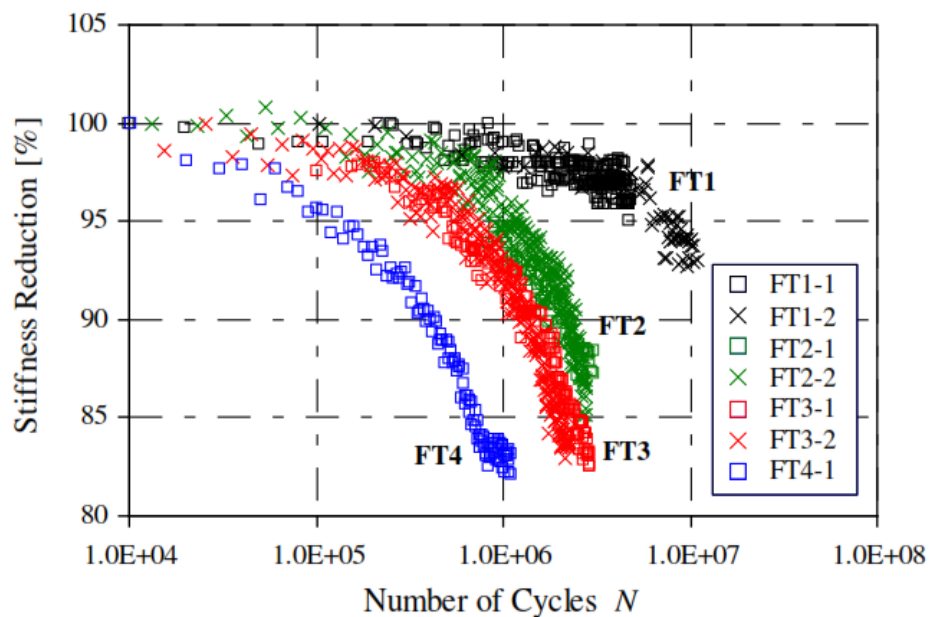


Figure 2.15: Reduction in stiffness of retrofitted specimens during fatigue tests. [6]

Colombi & Fava [35] prepared a series of steel/CFRP double shear lap joints using two steel plates and two CFRP strips and tested at different loading conditions defined as a function of stress range of 60, 75, 90 and 100 MPa, and of the stress ratio  $R$  (0.1 and 0.4). Significant stiffness reduction of the joints was first observed due to progressive debonding of CFRP strips. Similar to Bocciarelli et al. [6], crack initiation is associated to 2% stiffness reduction and 5% reduction when the debonding propagates more rapidly. When it reached 10% stiffness reduction, it is when the final failure took place. They suggested considering the stiffness reduction to 98%, 95% and 90% when developing the S-N curves from the test results to assess the fatigue behavior of the bond between the steel plates and the CFRP strips. The tests evidenced a marginal influence of the fatigue ratio  $R$  on the fatigue performance.

#### **2.4.4 Stress range effect**

Deng & Lee [36] carried out a series of small-scale steel beams bonded with CFRP plate. Using backface-strain technique to detect crack initiation and monitor crack growth, it is proven that the crack nucleation and growth rate increased rapidly with the increment in applied stress range. In addition, the spew fillet is observed to be beneficial to the fatigue performance of the adhesively bonded joints but not significant. An S-N curve was developed from the test results and the fatigue limit was found to be about 30% of the ultimate static failure stress, which validates the fatigue limit suggested by CIRIA Design Guidance [37]. Also, the fatigue load range will affect the fatigue life, but its significance is much less than the magnitude of the maximum load in the load range.

Kim & Harries [38] on the other hand, intentionally created damage by notching the tension flange of the six beams to evaluate the static and fatigue performance when the specimens are repaired with CFRP strips. From the tests, recovery of the static load-carrying capacity of the damaged beam to the undamaged beam is observed with the use of CFRP strips. In addition, the stress range applied was found to be the governing factor for fatigue life of the repaired beam with results as shown in Table 2.12 where higher stress range yield lower fatigue life of the flange. A bilinear fatigue response is observed at the CFRP-steel interface, whose magnitudes are dependent upon the number of fatigue cycles and the applied stress range. An empirical model was also proposed to predict the fatigue behavior of the interface.

Table 2.12: Beam details and test results [38]

Specimen	Method	$\Delta\sigma$ (MPa)	Fatigue life
<b>Beam D</b>	Experimental	274	20000
	Finite Element Analysis	274	15000
<b>Beam E</b>	Experimental	158	152380
	Finite Element Analysis	158	150000
<b>Beam F</b>	Experimental	81	1703020
	Finite Element Analysis	81	2100000

Different approach was used by Imanaka et al. [39] to study the key parameter governing the fatigue strength of adhesive-bonded CFRP pipe/steel rod joints. A series of rotating bending fatigue tests was carried out with different bond length and pipe thicknesses. From the experiments, it was found that the rotating bending fatigue strength increases with lap length as shown in Figure 2.16. Also, the fatigue strength increase consistently with the pipe thickness but only in low stress cycle range. The results indicated that the fatigue strength of the joint mainly depended on the maximum tensile stress normal to the adhesive interface at the lap end.

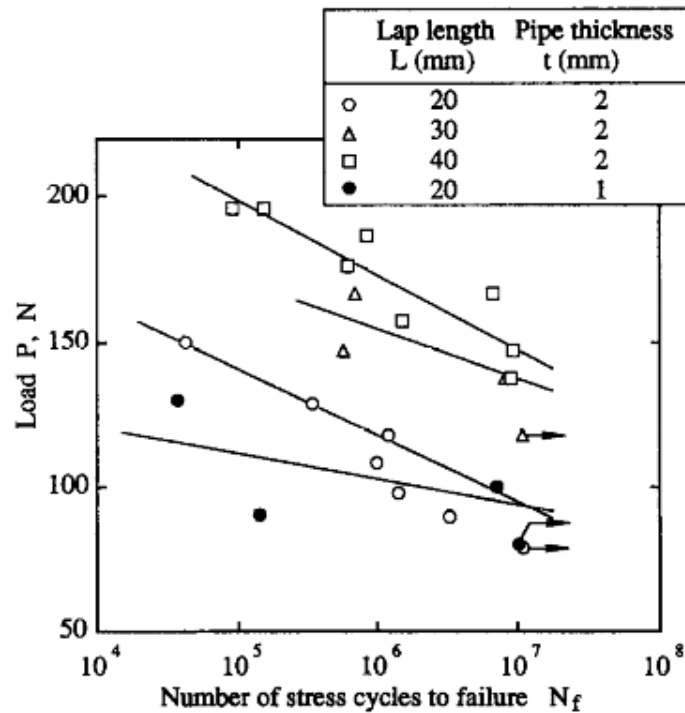


Figure 2.16: Results of fatigue test (P-N curves) [39]

## 2.5 EFFECTIVE BOND LENGTH

The bond is crucial in order to successfully transfer the load between the CFRP and steel interfaces. However, an appropriate bond length is needed; too short bond length will not be able to cater the load transfer while longer bond does not ensure more significant load transfer. Hence, here comes the need to determine the effective bond length that produces the maximum possible stress in the CFRP [19]. Effective bond length simply means the shortest bond length that maximizes the load transferred into the CFRP plate.

Few researches have been carried out in order to determine the effective bond length of CFRP plated steel member. Anyfantis & Tsouvalis [40] in their study, focused on the effect of adhesive thickness, stiffness ratio and overlap length to the stiffness and strength of the joint. From the result, the failure loads are not that sensitive with regards to the adhesive thickness and load ratio. 70% increase in adhesive thickness lead to 5% or 13% increase in strength with 25mm and 75mm overlap length respectively. Whereas, 100% increase in load ratio only resulted in 5% maximum increase in strength. However, the joints with three times longer overlap (200% increases) yielded a 100% maximum increase in their strength, compared to the joints with short overlap lengths.

Table 2.13: Geometry and dimensions of the fabricated coupons [40]

Specimen	Overlap Length, $L_o$ (mm) (75/25)	Adhesive Thickness, $t_a$ (mm) (0.5/0.85)	Average Shear Strength, $\tau_s$ (MPa)	Failure Load, $P_{max}$ (kN)
SLJ-1	75	0.52	10.7	19.1
SLJ-2	75	0.89	12.2	22.0
SLJ-3	75	0.51	10.7	19.2
SLJ-4	75	0.84	12.2	21.9
SLJ-5	25	0.51	13.4	8.0
SLJ-6	25	0.85	13.5	8.1
SLJ-7	25	0.50	14.1	8.5

*SLJ refers to Single Lap Joint. Adhesive: Araldite 2015*



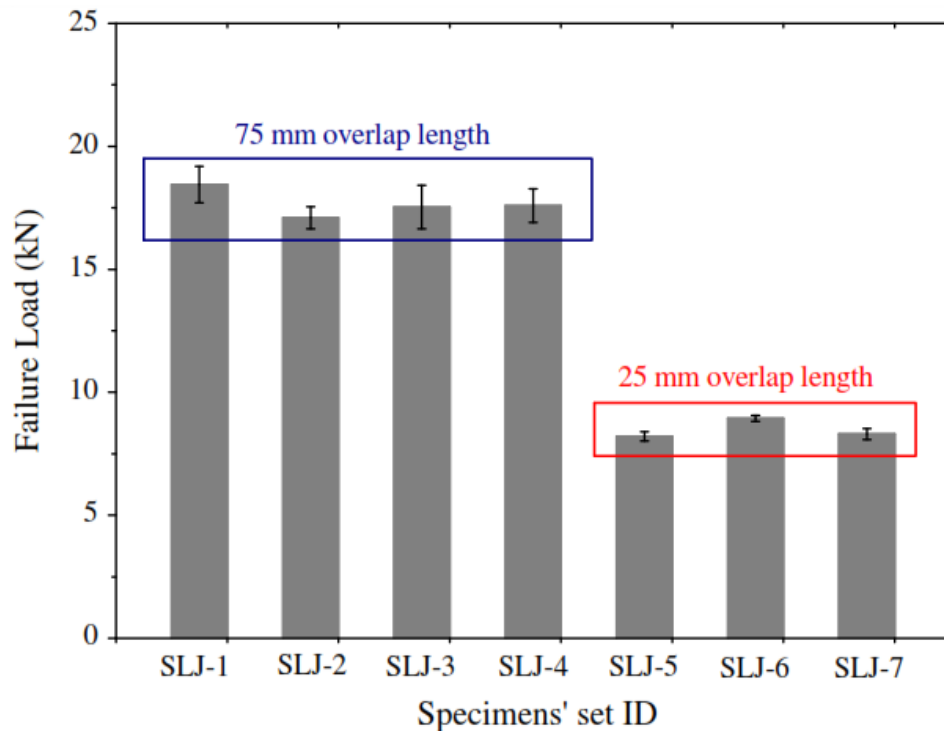


Figure 2.17: Experimental failure loads of all seven SLJ cases tested. [40]

Wu et al. [2] on the other hand compare the experimental results with previous researches. Two different adhesive were used, Araldite 420 (tensile strength 28.6 MPa) and Sikadur 30 (tensile strength 24 MPa). Both adhesive shows that the bond strength increase with the bond length. From the plotted bond strength and bond length relationship, it can be seen that the effective bond lengths for Araldite 420 and Sikadur 30 are about 110mm and 85mm respectively. This is most likely because Araldite is more ductile than Sikadur, leading to a longer shear stress distribution within the bond length.

Table 2.14: Results of double strap joints [2]

<b>Specimen</b>	<b>Bond Length (mm)</b>	<b>Adhesive Thickness, <math>t_a</math> (mm)</b>	<b>Ultimate Load <math>P_{ult}</math> (kN)</b>
<b>A260</b>	260	0.39	274.95
<b>A250</b>	250	0.38	267.34
<b>A120</b>	120	0.36	271.18
<b>A100</b>	100	0.31	250.63
<b>A70</b>	70	0.34	178.88
<b>A50</b>	50	0.36	137.23
<b>A30</b>	30	0.35	72.97
<b>S250</b>	250	0.43	151.33
<b>S100</b>	100	0.40	148.42
<b>S80</b>	80	0.35	158.07
<b>S70</b>	70	0.40	126.44
<b>S50</b>	50	0.43	136.35
<b>S30</b>	30	0.34	58.51

*'A/S' refer to adhesive type (Araldite/Sikadur)*

Also, they presented the comparison of effective bond lengths of steel joints with CFRP sheets, normal modulus CFRP and UHM CFRP laminates as tabulated in Table 2.15.

Table 2.15: Effective bond lengths of different CFRP-steel systems [2]

<b>System</b>	<b>CFRP Modulus</b>	<b>Effective Bond Length (mm)</b>
CFRP sheet-steel	240 GPa (Normal Modulus)	75
(Fawzia, S.) [41]	640 GPa (High Modulus)	40
CFRP laminate-steel	165 GPa	104mm similar to Araldite
(Xia & Teng) [4]		82mm similar to Sikadur
UHM CFRP	460 (GPa)	110mm for Araldite
laminate-steel		85mm for Sikadur

Clearly from the comparison, the effective bond length for CFRP sheet steel system is relatively shorter than of high modulus CFRP sheet.

Fawzia, Al-Mahaidi & Zhao [41] used 4 normal modulus CFRPs in their study with Araldite 420 (tensile strength of 32 MPa) as the adhesive.

Table 2.16: Results of specimen testing [41]

Specimen	Bond Length (mm)	Ultimate Load $P_{ult}$ (kN)
SN40	40	49.9
SN50	50	69.8
SN70	70	80.8
SN80	80	81.3

The ultimate load carrying capacity against the bond length is plotted and it can be seen that the load carrying capacity reaches a plateau after the bond length exceeds a certain value as shown in Figure 2.18. In this case, a bond length above 72mm will not result in any increment in the load carrying capacity. Hence, the effective bond length of 75mm is adopted in the experiment.

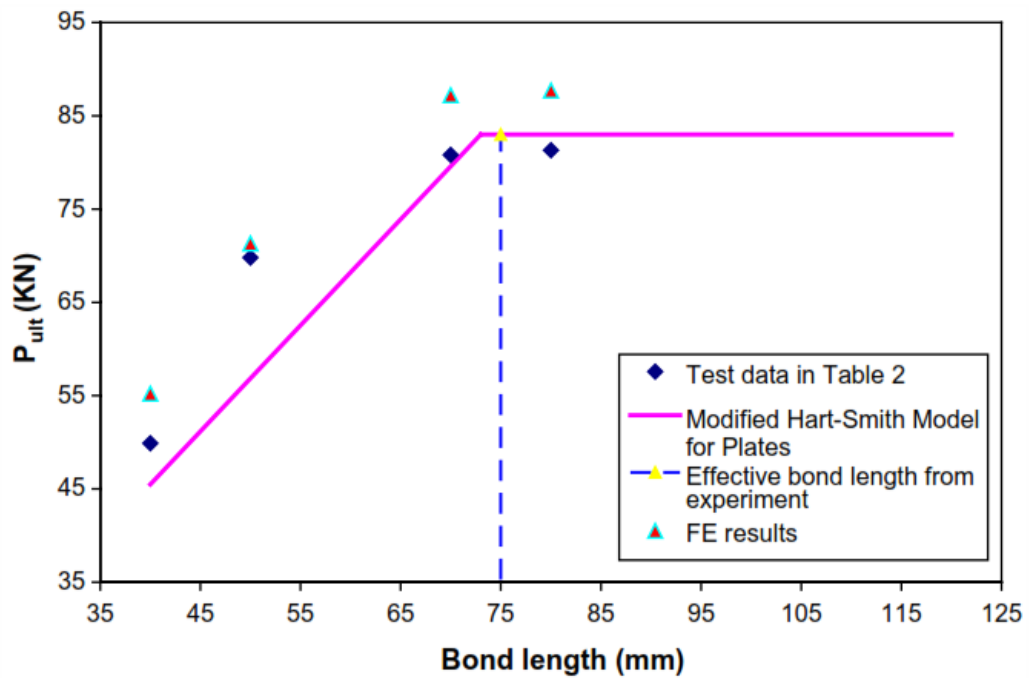


Figure 2.18: Effective bond length for normal modulus CFRP joint. [41]

In his analysis, Majid [42] studied the effect of different parameters on the effective bond length. These parameters include CFRP sheet thickness, adhesive layer thickness, steel plate thickness and number of CFRP layers. Using finite element analysis, the effect of two different CFRP sheet thicknesses was found to exhibit similar behavior on the effective bond length. Hence, the CFRP sheet thicknesses have no significant impact on the critical bond length. The same observation was made to the effect of steel plate thickness. Results show that no significant effect on the effective bond length when two thicknesses of steel plate were used, 5mm and 10mm. Contrary to adhesive thickness, it has a significant effect, where the slip is found to be directly proportional to adhesive thickness.

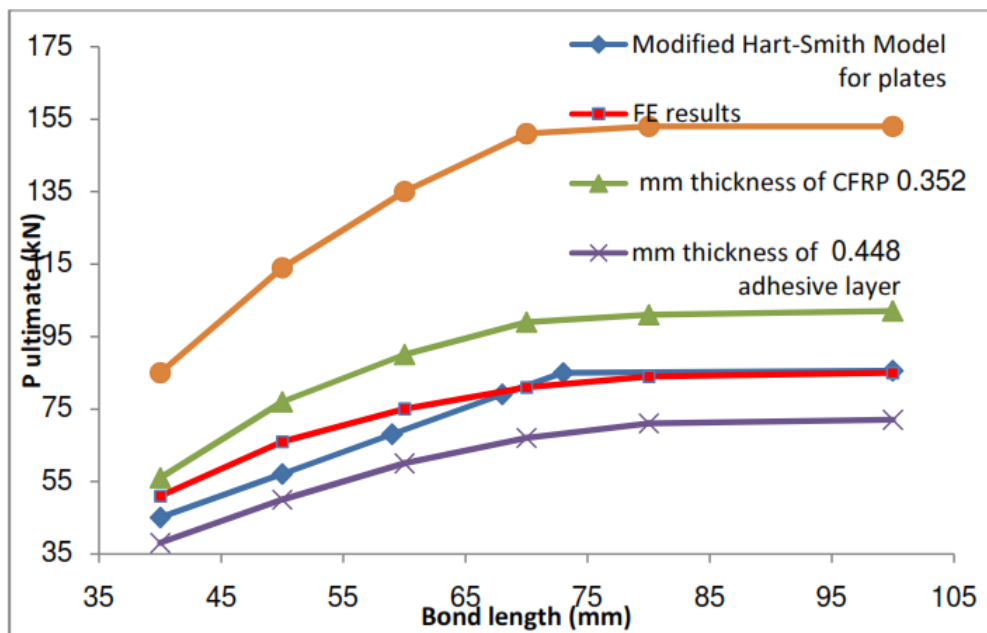


Figure 2.19: Effective bond length for CFRP joint. [42]

When different numbers of CFRP sheets used with same tensile strength and the sheet thickness, it shows a little effect on the effective bond length as shown in Figure 2.20. When one or two layers of CFRP sheets are used, the effective length increase to 80mm; and decreases to 75mm when 3 layers are used. The using of more than three layers reduces the effective length to 70mm.

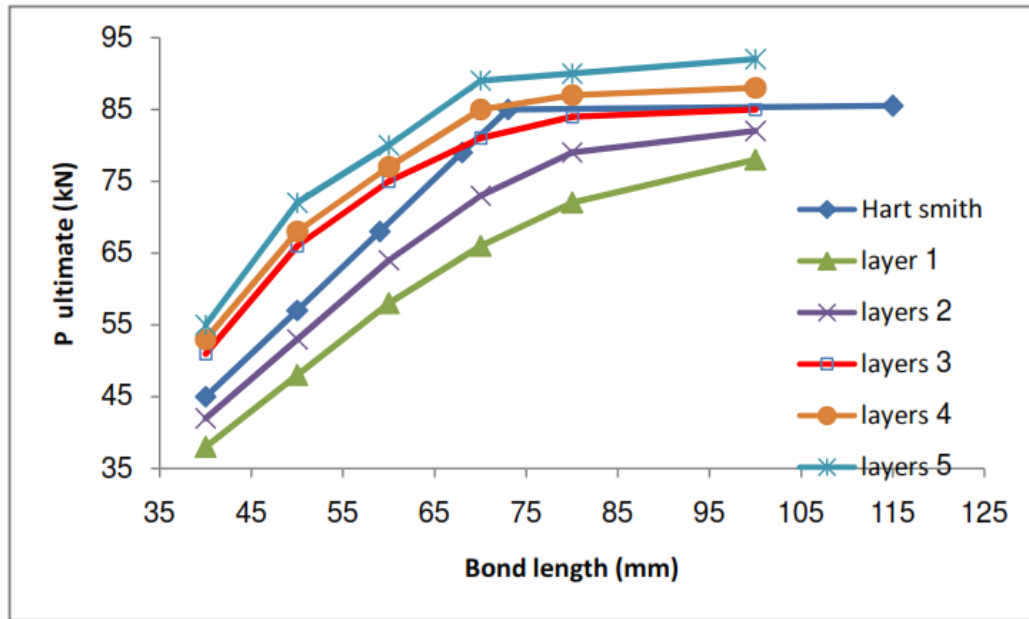


Figure 2.20: Effect of CFRP sheet layers number on effective bond length [42]

Fawzia & Karim [16] on another study, predict the bonding strength by plotting the experimental results with comparison to the imperial model developed using stress based approach:

$$P_{ult} = .8\tau w l_{eff}$$

where  $\tau$  is the shear stress of 28MPa and  $w$  is the width of the bonding area.

Table 2.17: Test results [43]

Specimen	Bond Length (mm)	Ultimate Load $P_u$ (kN)
NA20	20	33.7
NA40	40	49.9
NA50	50	69.8
NA60	60	58.8
NA70	70	80.8
NA80	80	81.3
NA90	90	69.8
NA150	150	91.0
NA200	200	92.6

<b>NA250</b>	250	97.2
--------------	-----	------

Figure 2.21 shows quite a good agreement of the imperial model with the experimental results. From the plotted graph, similar trend is observed, where after a certain bond length is reached, a plateau is produced and in this case, the plateau is observed to form after 70mm of bond length is exceeded. Further increase in the bond length does not bring any significant to the load carrying capacity.

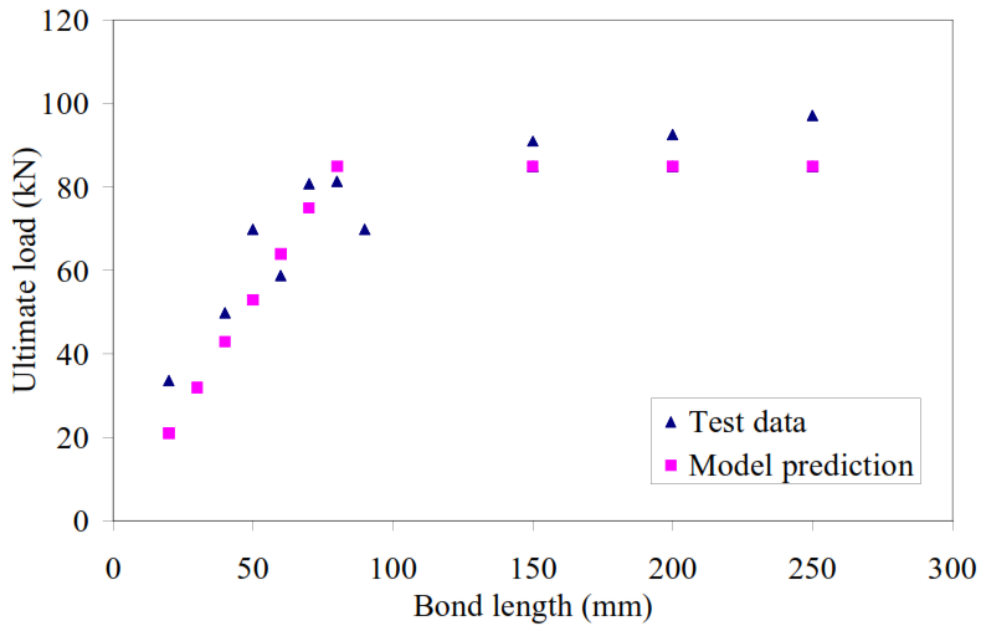


Figure 2.21: Comparison of experimental and imperial model result [43]

Nozaka, Shield & Hajjar [19] used fatigued steel bridge I-girders with five different configuration of test set up to achieve wide range of result as well as to modify and relieve the stress concentration in the adhesive when sharp corners exist in the adhesive layers. 27 specimens were tested; 23 were of one layer CFRP, three specimens were two layers and one specimen was three layers.

Table 2.18: Material properties [19]

Strip/Adhesive		Modulus of Elasticity (GPa)	Tensile Strength (GPa)
<b>CFRP Strip</b>	1. Carbodur	157	2.6
	2. Tyfo UC	114	0.79
<b>Adhesive</b>	A. Sikadur 330	4.6	41
	B. Sikadur 30	-	25
	C. Plus 25	-	17

D. DP-460 NS	1.8	35
E. Tyfo TC	-	47

From Table 2.19, for the specimen 1-3 and 1-4 which have the very same test arrangement except for the bond length, it shows no variation in the peak moment as well as the strain at failure when the bond length increased 170%. When much lower bond length of 203mm is used for specimen 1-7a, 1-7b, 1-7c, 1-8a, 1-8b, 1-8c and 1-9, the peak moment increase as well as the strain at failure. Also, from specimen 1-14 and 1-15, increasing the bond length to about 100% does not increase the strength. Hence the value of 203 mm bond length is adopted as the maximum bound for effective bond length. However, the exact effective bond length is to be determined based on the measured tensile strain distribution, which is 178mm.

Table 2.19: Effective bond length specimen matrix and summary of test results [19]

Specimen	CFRP	Adhesive	Configuration	Bonded length (mm)	Adhesive thickness (mm)	Peak moment (kNm)	Strain at failure <sup>a</sup> ( $\mu\epsilon$ )	Failure mode
1-1	1	A	1	380	1.5	36	4,000	D
1-2	1	A	2	380	1.5	36	3,000	D
1-3	1	A	4	380	1.5	41	4,000	D
1-4	1	A	4	660	1.5	41	4,000	D
1-5a	1	A	3	380	1.5	56	5,000	D
1-5b	1	A	3	380	1.5	59	6,000	D
1-6	1	A	5	380	1.3	50	5,800	D,F
1-7a	1	A	5	203	1.3	75	8,800	D,F
1-7b	1	A	5	203	1.3	77	8,900	D,F
1-7c	1	A	5	203	1.3	45	5,000	D,F
1-8a	1	A	5	203	1.3	79	10,000	D,F
1-8b	1	A	5	203	1.3	72	7,700	D,F
1-8c	1	A	5	203	1.3	56	6,300	D,F
1-9	1	A	5	203	0.5	41	4,800	D
1-10	1	B	4	380	1.5	36	2,500	D
1-11a	1	D	5	203	0.5	76	9,700	D,F
1-11b	1	D	5	203	0.5	75	9,500*	D,F
1-11c	1	D	5	203	0.5	84	8,800*	D,F
1-12	1	C	5	203	0.5	72	9,300	D
1-13	2	D	5	203	0.5	99	13,000+	N.A.
1-14	2	D	5	406	0.5	108	12,000	D,F
1-15	2	D	5	203	0.5	113	14,000	D,F
1-16	2	E	5	203	1.3	95	12,000+	N.A.
2-1	1	A	4	380	1.5	81	3,500	D
2-2	1	A	3	380	1.5	104	4,500+	N.A.
2-2 (retested)	1	A	3	380	1.5	122	5,500	D
2-3	2	D	5	406	0.5	186	10,000	D
3-1	1	A	3	380	1.5	131	4,000	D

Note: CFRP=carbon-fiber-reinforced polymer; D=debonding; F=rupture of several fibers; and N.A.=not applicable.

\*=heat-cured; and +=terminated before failure.

## 2.6 MODES OF FAILURE

Most of recent previous researches carried out reported typical modes of failure expected in CFRP-to-steel adhesively bonded joints to be either adhesive failure or delamination and some reported CFRP rupture when UHM CFRP is used [2]. Zhao & Zhang [7] classified up to six failure modes for CFRP bonded steel joints namely: (1) steel and adhesive interface failure, (2) cohesive failure (adhesive layer failure), (3) CFRP and adhesive interface failure, (4) CFRP delamination (separation of some carbon fibers from the resin matrix), (5) CFRP rupture and (6) steel yielding.

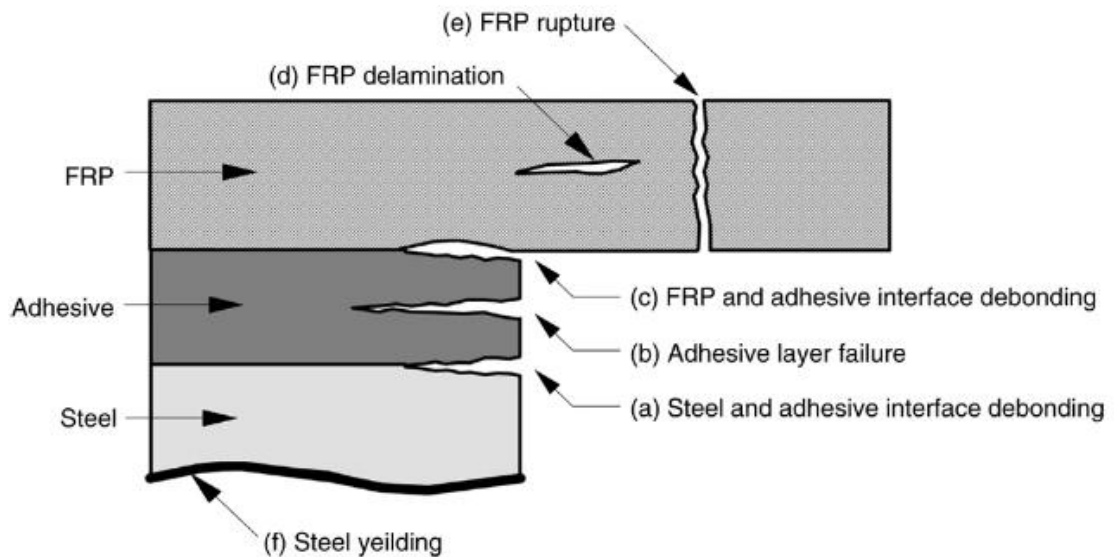


Figure 2.22: Schematic view of failure modes [7].

These modes of failure are well correlated with varying parameters adopted in each study such as modulus of elasticity of the CFRP, adhesive thickness and type of adhesive used. Thin application of adhesive usually results in adhesive failure and tends to shift towards CFRP delamination when higher thickness of adhesive is used [3]. CFRP rupture is most likely to occur when UHM CFRP is used [2, 3]. Steel yielding on the other hand, will occur when insufficient plate thickness is used in the testing [7].



## 2.7 BOND-SLIP RELATIONSHIP

Limited research has been conducted to study the bond-slip relationship of adhesively bonded CFRP-to-steel when subjected to fatigue loading. In contrast, much attention has been given to the bond-slip relationship analysis on concrete structures [1, 7].

Bond-slip relationship is a crucial characteristic to be analyzed when it comes to CFRP bonded steel or concrete systems. It is used to derive the effective bond length, bond strength and slip [44, 7]. Strain gauges installed at predetermined distances along the bond length are used to measure the axial strains and this parameter is used to derive the bond-slip relationship.

Using a single shear pull-off test in Figure 2.23, Xia & Teng [4] proposed a simple bilinear bond-slip model based on the shear bond stress-slip plot from the experiments conducted as shown in Figure 2.24. Strain gauges were installed on the CFRP plates to monitor and measure the instantaneous slip and to deduce the interfacial shear stresses.

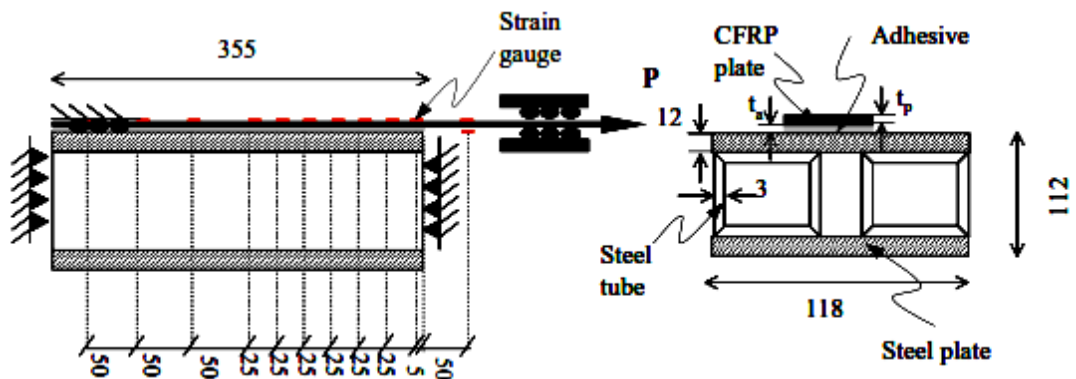


Figure 2.23: Pull-off test set up [4].

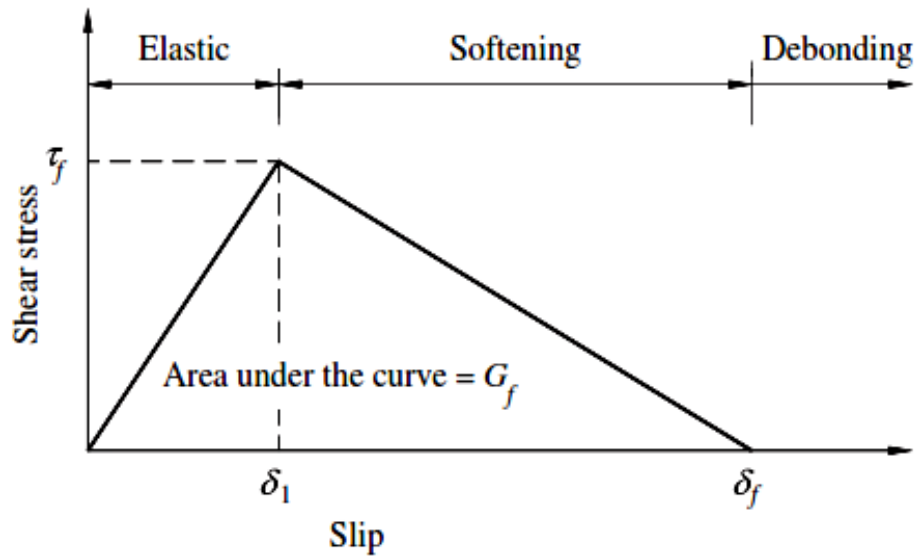


Figure 2.24: Bilinear bond-slip model [4].

Nevertheless, a new bond-slip model was proposed by Dehghani et al. [45] where the addition of plastic part to the conventional bilinear model is done as shown in Figure 2.25. Previous bond-slip models portray non-conformities with experimental results, particularly in elastic part and elastic properties of the adhesive. This is due to the fact that the strain gauges are installed on CFRP surface instead of adhesive surface hence interfacial stresses and strains showed some errors [4].

From the new model, the maximum shear stress in the adhesive ( $\tau_f$ ) is estimated to be about 80% of maximum tensile strength ( $f_{t, a}$ ). The slope of ascending part of the proposed bond-slip curve is calculated based on elastic properties of the adhesive. Also, it is important to note that there is not clear relationship between the interfacial fracture energy,  $G_f$  and other adhesive properties such as thickness. This new proposed model is able to consider the initial stiffness of the joints, and to estimate the ultimate debonding load and effective bond length with good accuracy.

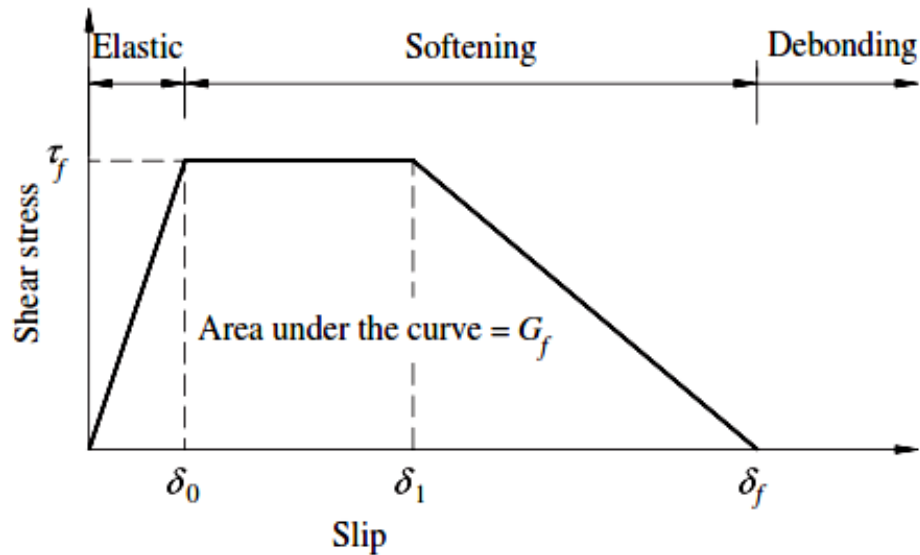


Figure 2.25: New proposed bond-slip model by Dehghani et al. [45].

## 2.8 CONCLUSION

Considering all the studies carried out by most of the researches, it is deducible that most of them solely focus on the bond behavior of the CFRP/steel joints subjected to static tensile loading, impact loading or fatigue loading. Nevertheless, none of the researches have reported the establishment of bond-slip relationship in CFRP plated steel members subjected to fatigue loading, which is the main focus of this research.

In addition, there is no established fatigue loading testing regime for CFRP plate steel member. A good fatigue loading range is crucial to see the full range behavior of this composite system and to produce the intended S-N curve and bond-slip relationship.

A single strap pull test will be used in this research since it is the best testing configuration to see the bond behavior of this composite system as suggested by Zhao & Zhang [2].



## CHAPTER 3

### METHODOLOGY

A number of methods and procedure should be taken into consideration to reassure the intended objectives of this study will be accomplished. All the data obtained will be gathered and analyzed in detailed to obtain the expected end result. The methodology approach used in this study is presented in this chapter.

#### 3.1 RESEARCH METHODOLOGY

##### 3.1.1 Literature review

In every study carried out by most of researchers, this is the early and crucial stage that should be given special attention such that from this stage, overall overview of the proposed topic of study is formed. At this stage, documentation research is implemented where relevant references such as books, journals, conference proceedings, articles and sources from internet are to be sought. This stage is very important in order to help the author to find related resources that will assist to cover the planned research scope.

##### 3.1.2 Experimental program

In this study, experiment is carried out in order to obtain data and subsequently deliver the intended objectives of the study. For the purpose of this research, a single strap pull test will be carried out to study the behavior of the composite system. The obtained data will also be used in the fatigue life prediction. Basic properties of the adhesive and CFRP plate are tabulated in Table 3.1.

Table 3.1: Material properties.

Material	$S_u$ (MPa)	$E_a$ (GPa)	Strain at Break (%)
Adhesive Sikadur 30	24.8	4.482	1.1
CFRP Sika Carbodur S	3100	165	1.7

### *Preparation of the steel block*

1. The steel block is formed by welding two 12 mm thick steel plates to two 70 mm by 50 mm rectangular hollow sections of 3 mm in thickness.
2. To enhance the bonding capability, the two test surfaces (top and bottom) will be sandblasted and cleaned with acetone to remove any dirt, rust and residues as shown in Figure 3.1.



Figure 3.1: Steel blocks after being sandblasted.

3. Ball bearings of 1 mm diameter will be glued to the steel surface with a tiny drop of adhesive to keep them in place. (Figure 3.2)

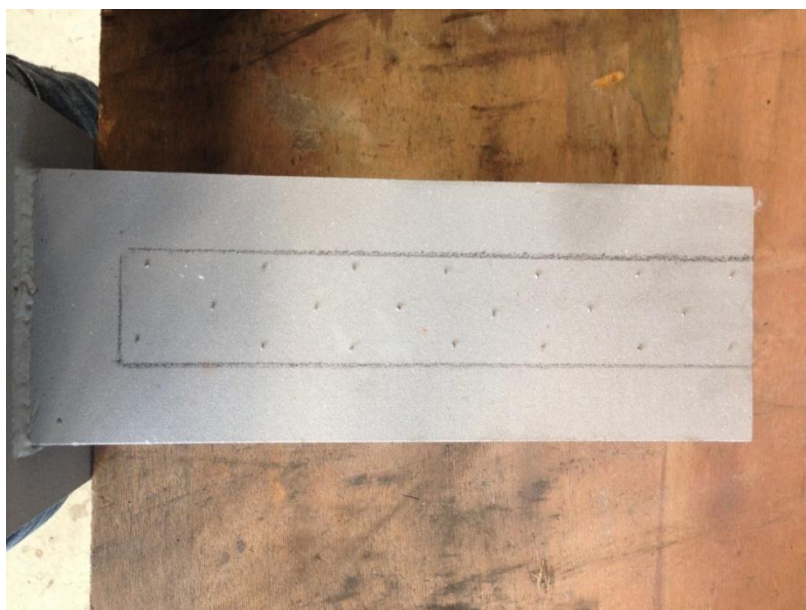


Figure 3.2: Ball bearing glued to the steel surface.

4. The adhesive is then prepared by using Sikadur 30 by mixing the Part A and Part B. A ratio of 3:1 is used respectively.



Figure 3.3: Sikadur 30 Part A and Part B.



Figure 3.4: Mixing the adhesive.



5. After the adhesive had been laid out, the CFRP plate will be pressed down, squeezing out excessive adhesive out, to provide both an even surface and adhesive thickness of 1 mm. A weight will then be placed on top of the CFRP plate for seven days whilst curing.



Figure 3.5: Placing weight on top of the CFRP plate.

6. A series of 15 strain gauges are installed along the centre line of the CFRP plate using adhesive.

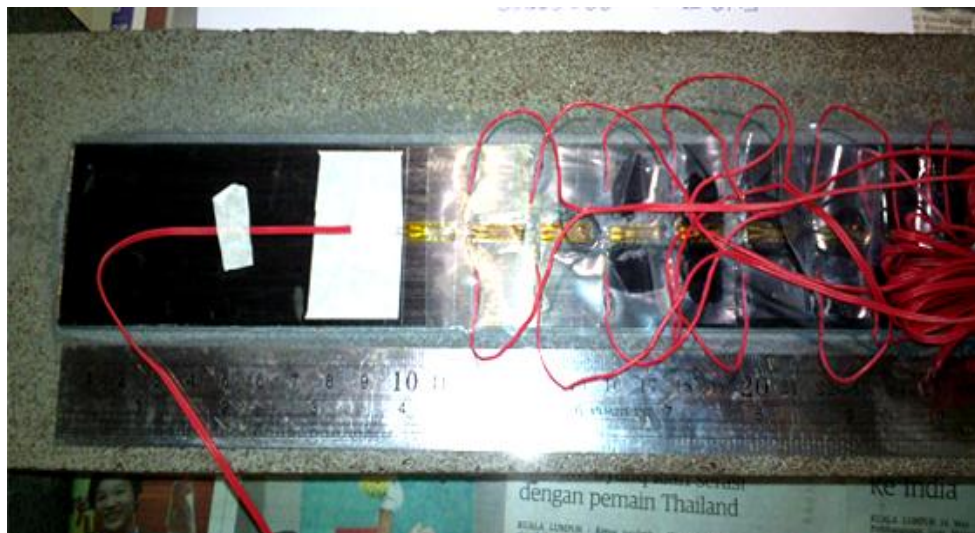


Figure 3.6: Installation of strain gauges along the CFRP plate.



### Single Strap Pull Test

The cured specimen will then be mounted to the Universal Testing Machine (UTM) for testing. A loading rate of 0.005 kN/s is used throughout the testing. The CFRP plate will be pulled upwards and the strains and slips will be recorded at the frequency of 1 Hz. The elastic modulus will be measured directly from the strain gauges on the unbounded part of the CFRP plate in the pull tests, as shown in the Figure 3.7.

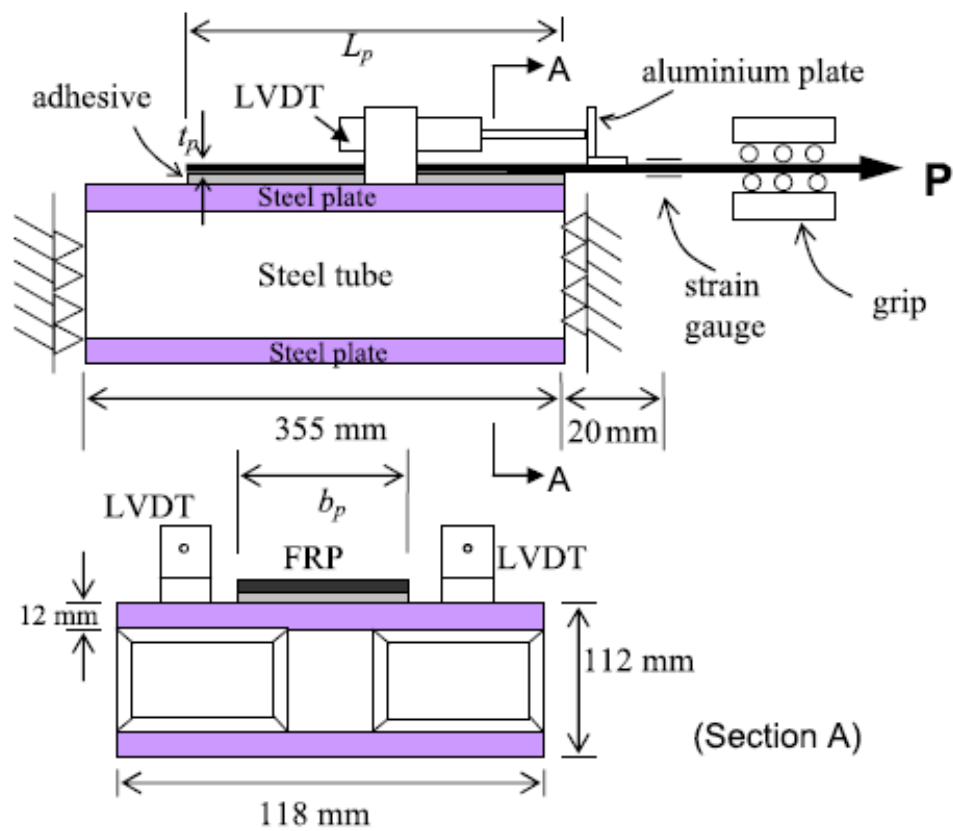


Figure 3.7: Single strap pull test specimen setup.

#### 3.1.3 Data collection and analysis

Raw data from the UTM after the testing are carried out will be extracted and analyzed with respect to the scope of study; behavior and shear stress distribution along the bonded length. In this stage, the data will be processed one by one and will be prepared to be presented in simpler manner such as charts and tables. The results will be compared to the theoretical and established bond-slip model and stress distribution along the bonded length by Xia & Teng [4].

### **3.1.4 Fatigue life prediction using Stress-Life approach**

Using the data from the experiment, a suitable load range for the fatigue loading program will be determined. This is to ensure the provision of good groundwork for the fatigue study of this composite system in the later stage. The load range determination was calculated by predicting the fatigue life using the stress-life approach [46]. Using this approach, the S-N curve can be predicted for this composite system. Further calculations and discussions are presented in Chapter 4: Result and Discussion

### 3.2 PROJECT ACTIVITIES

In order to achieve the intended objective of the research and to ensure good progress and correct path of the study, the following research methodology flow chart is produced (Figure 3.8).

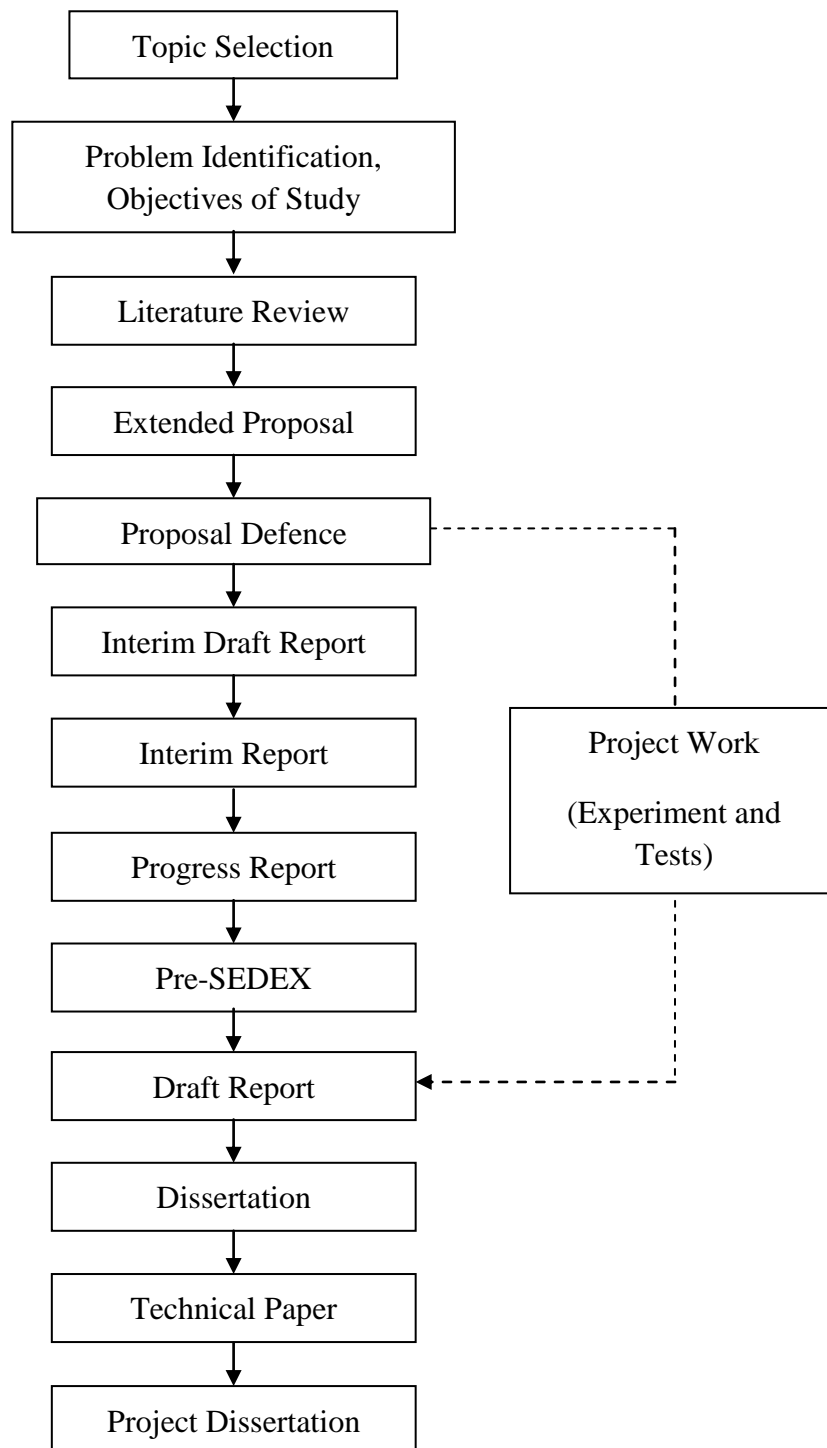


Figure 3.8: Planned project activities.

### 3.3 KEY MILESTONE AND GANTT CHART

Table 3.2: Gantt Chart of the research project.

Detail/Week		1	2	3	4	5	6	7		8	9	10	11	12	13	14	
<b>FYP 1</b>	Selection of Project Topic	Yellow	Yellow						<b>Mid-Semester Break</b>								
	Preliminary Research Work		Yellow	Yellow	Yellow	Yellow											
	Submission of Extended Proposal Defense						Red										
	Proposal Defense										Yellow	Yellow					
	Project work continues												Yellow	Yellow	Yellow		
	Submission of Interim Draft Report															Red	
	Submission of Interim Report																Red
<b>FYP 2</b>	Project Work Continues	Yellow	Yellow	Yellow	Yellow	Yellow	Yellow	Yellow	<b>Mid-Semester Break</b>								
	Submission of Progress Report										Red						
	Project Work Continues										Yellow	Yellow	Yellow	Yellow			
	Pre SEDEX												Red				
	Submission of Draft Report													Red			
	Submission of Dissertation (Soft Bound)														Red		
	Submission of Technical Paper														Red		
	Oral Presentation															Red	
	Submission of Project Dissertation (Hard Bound)																Red

**Process**

### **3.4 TOOLS AND EQUIPMENTS**

In order to facilitate this study, few tools and equipments are to be used throughout the research program.

1. Microsoft Office 2007
2. Carbon Fiber Reinforced Polymer (CFRP)
3. Steel blocks
4. Universal Testing Machine (UTM)
5. Adhesive (Araldite and Sikadur 30)
6. Cutting tools and machine
7. Personal Laptop and Compact Digital Camera



## CHAPTER 4

### RESULTS AND DISCUSSIONS

In this chapter, results from the experimental program on specimen as well as fatigue life prediction are presented in relevant tables and graphs. Discussions on the analyzed results are further elaborated in depth with comparisons to relevant findings by other researches.

#### 4.1 BEHAVIOUR OF CFRP PLATED STEEL MEMBER AND SHEAR STRESS DISTRIBUTION ALONG THE BONDED LENGTH

##### 4.1.1 Failure mode

The failure mechanism was observed to initiate with CFRP debonding at the loaded end and propagate along the interfaces until failure completely occur as shown in Figure 4.1. The specimen failed along the CFRP-to-steel interface with a wedge of adhesive on the CFRP plate near the loaded end. Also, cracks were observed to propagate along the CFRP plate which strongly portrayed that the adhesive interfaces might be stronger than interfaces between the resin matrix within the CFRP plate (Figure 4.2).

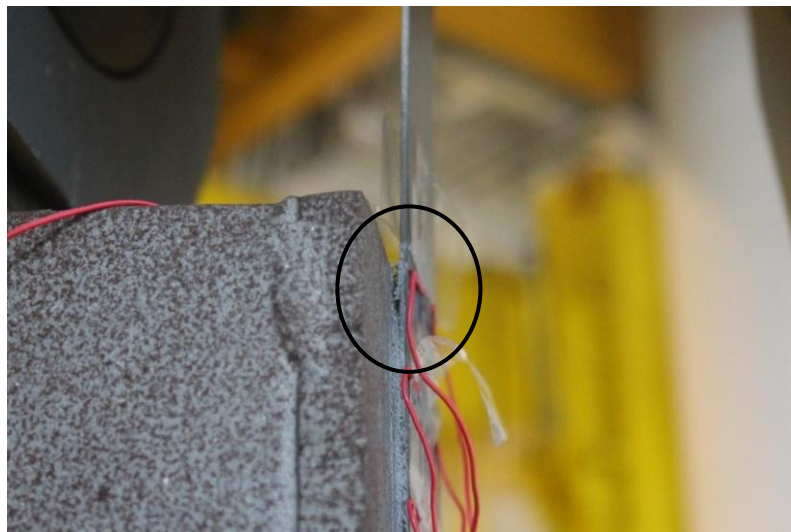
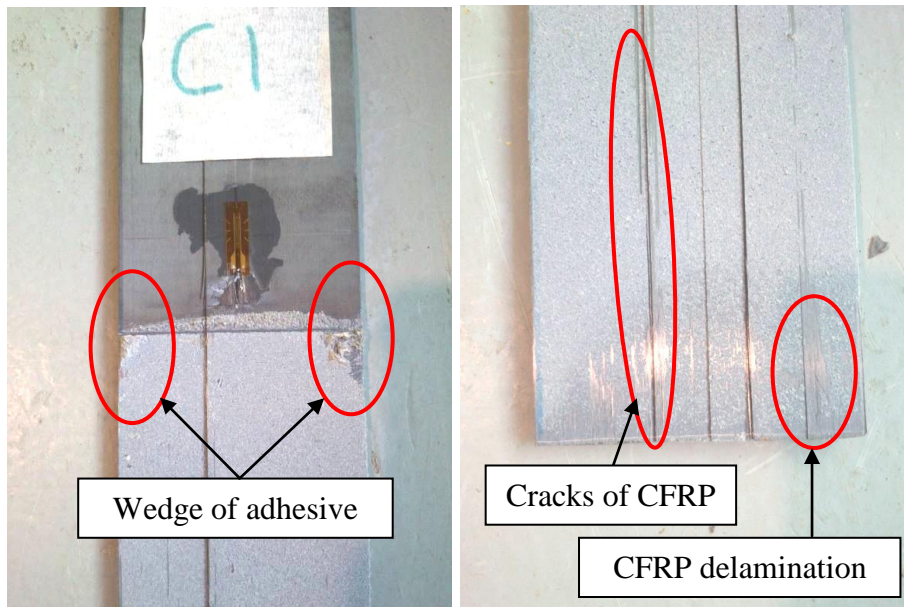


Figure 4.1: Debonding first occurred near the loaded end.



(a) Overall failed specimen.



(b)

(c)

(b) Wedge of adhesive observed near the loaded end. (c) Cracks of CFRP in longitudinal direction and some CFRP fiber delamination.

Figure 4.2: Failure mechanism of the control specimen.



### 4.1.2 Bond-slip Relationship

The bond-slip relationship is determined from axial strains measured with strain gauges along the bond length. The raw data; strain, applied load and stroke were first processed in a spreadsheet in order to come up with a meaningful result presentation. The example of the calculation using the spreadsheet is shown in Figure 4.3.

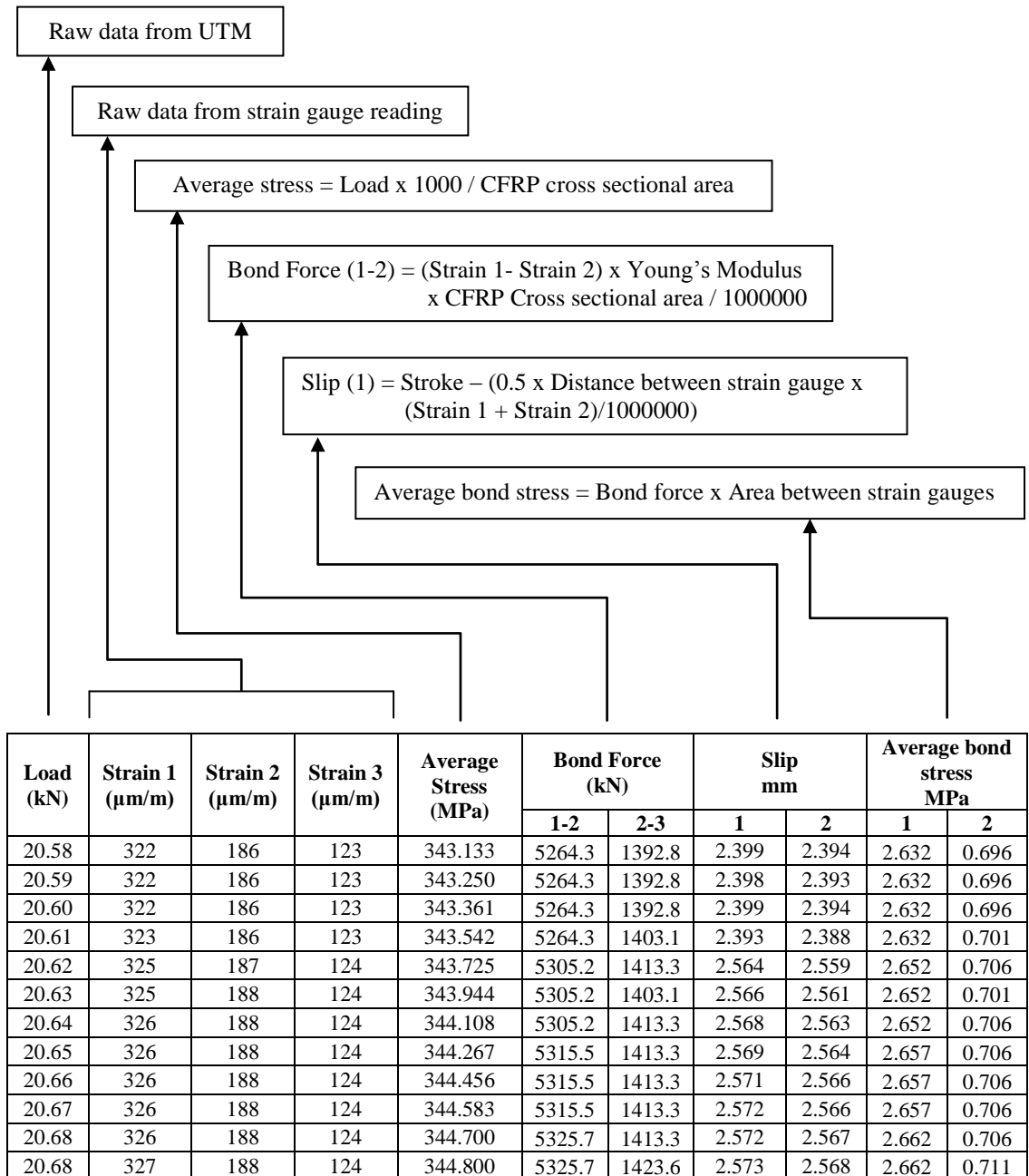


Figure 4.3: Sample spreadsheet calculation to process the raw data.

After all the data have been processed accordingly, the bond-slip relationship is plotted for each strain gauge distance, using the value of slip and average bond stress. The bond-slip relationship for the control specimen is shown in Figure 4.4.

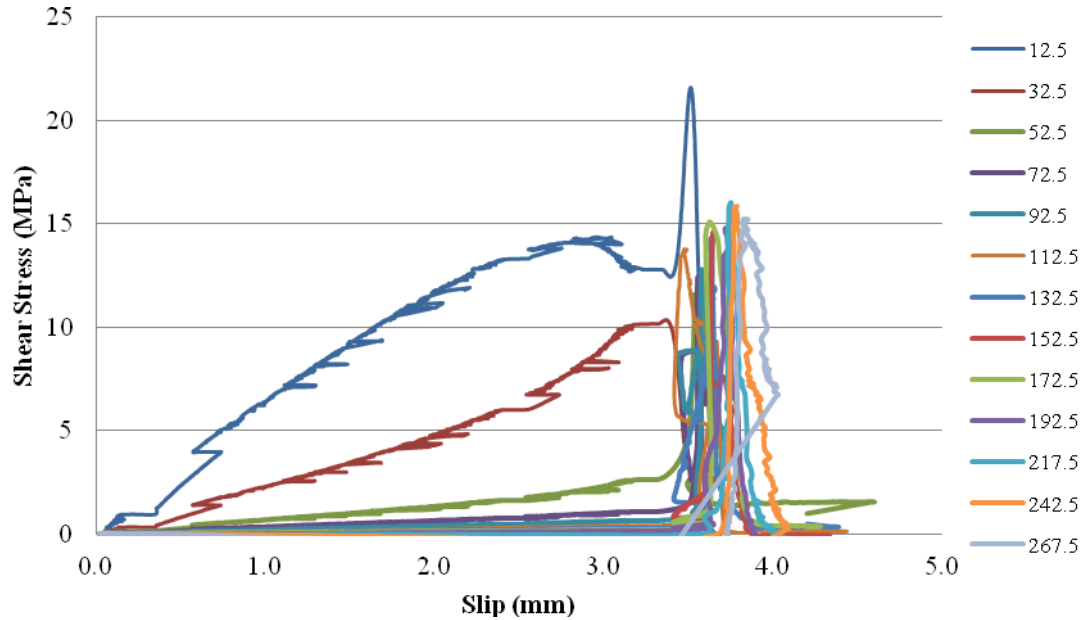


Figure 4.4: Bond-slip relationship for control specimen.

Figure 4.4 shows that the bond-slip relationship model for the control specimen does not conform to the bilinear model as suggested by Xia & Teng [4]. Only for the first point, 12.5 mm shows a good development of bilinear shape of the bond-slip relationship, however, there is a slight decline in the shear stress before sudden surge up to 21.6 MPa. This might be due to the micro cracking happening in the adhesive interface just before that specific point achieved the maximum stress. The bond-slip relationship should have similar shape for every location except near the loaded end, where the higher strain readings are expected to have been affected by local bending of the plate.

### 4.1.3 Load-Displacement behavior

Figure 4.5 shows the load-displacement curve for the control specimen. From the experimental result as shown in blue line, it can be seen that there is some irregularity in the curve as it seems not be as linear as the theoretical shape shown in red line. This might be due to the micro-cracking that is taking place within the adhesive layer as suggested by Xia & Teng [4].

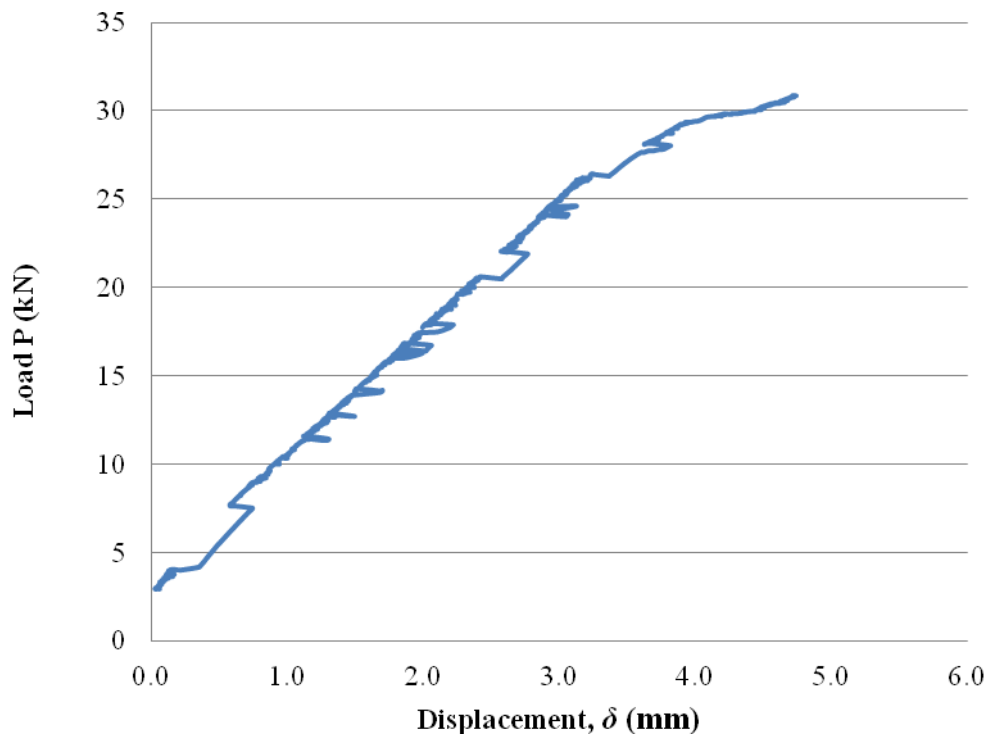


Figure 4.5: Load-displacement curve.

### 4.1.4 Shear stress distribution along CFRP-Steel interface

Figure 4.6 shows the distribution of shear stress along the CFRP-steel interface at different load levels. These shear stresses were calculated from the readings of strain gauges installed along the CFRP plates. As discussed by Xia & Teng [4], these values represent the average shear stress over the strain gauge intervals and are thus smaller than the actual values in the specimen.

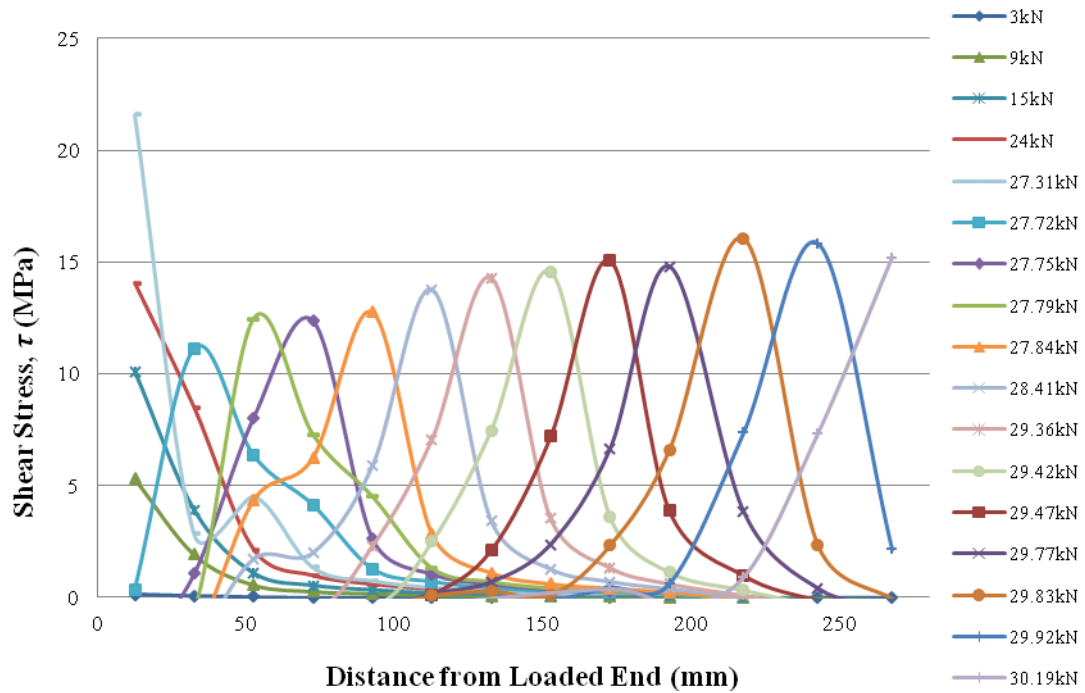


Figure 4.6: Shear stress distributions.

The graph in Figure 4.6 explains that at lower load level, shear stress was found largest near the loaded end and gradually reduced to zero towards the unloaded end. As the load increased, the shear stress approached the local bond strength or the maximum interfacial shear stress. When the loaded end reached the local bond strength at 27.31 kN load level, the CFRP-steel interface entered its softening stage during which the shear stress at the loaded end gradually decreased afterwards.

Subsequently, the shear stress at the loaded end reduced to zero where the ultimate load of the specimen is reached and debonding started to propagate along the interface. This happened when the load is slightly increased to 27.72 kN. From Figure 4.6, it can be seen that the peak shear stress moves away from the loaded end with only small increment in load level. The shear stress distribution of this specimen was found consistent as those described by Xia & Teng [4].

The peak shear stresses should not vary much along the bond length. However, the highest peak shear stress near the loaded end (21MPa) is believed to have been affected by the local bending of the CFRP plate.

## 4.2 FATIGUE LIFE PREDICTION USING STRESS-LIFE APPROACH

In order to predict at which stress level and when the specimen will fail during the fatigue testing later, fatigue life prediction is done beforehand. In this approach, several parameters are found to have great impacts on the fatigue life of the specimen. Using stress-life approach, the number of cycles as well as fatigue strength at failure can be predicted beforehand. The experimental data obtained from the control specimen testing in the first stage is used for this calculation.

Finite Life Modified Goodman:

$$\frac{S_a}{S_{Nf}} + \frac{S_m}{S_u} = 1 \quad (1)$$

where

$S_a$  is alternating stress

$S_{Nf}$  is fatigue strength at failure

$S_m$  is mean stress

$S_u$  is ultimate tensile strength

Basquin's Equation:

$$S_{Nf} = A(N_f)^B = S_u(N_f)^B \quad (2)$$

or

$$S_f = S_u(10^6)^B$$

Ultimate tensile load = 30.876kN (Based on static tensile test)

$$\begin{aligned} \text{Area} &= 1.2\text{mm} \times 50\text{mm} \\ &= 60\text{mm}^2 \end{aligned}$$

$$\begin{aligned} S_u &= \frac{30876\text{N}}{60\text{mm}^2} \\ &= 514\text{MPa} \end{aligned}$$

$$S_f = x(514\text{MPa})$$

$X$  is the coefficient of endurance limit,  $S_f$ . The coefficient of most metals falls under the range 0.2-0.5. However, no established endurance limit for adhesive bonded composite. Hence, few graphs have been plotted using different value of this coefficient to see the effects on the S-N curve as shown in Figure 4.7.

### Effect of Endurance Limit Coefficient on Fatigue Cycles

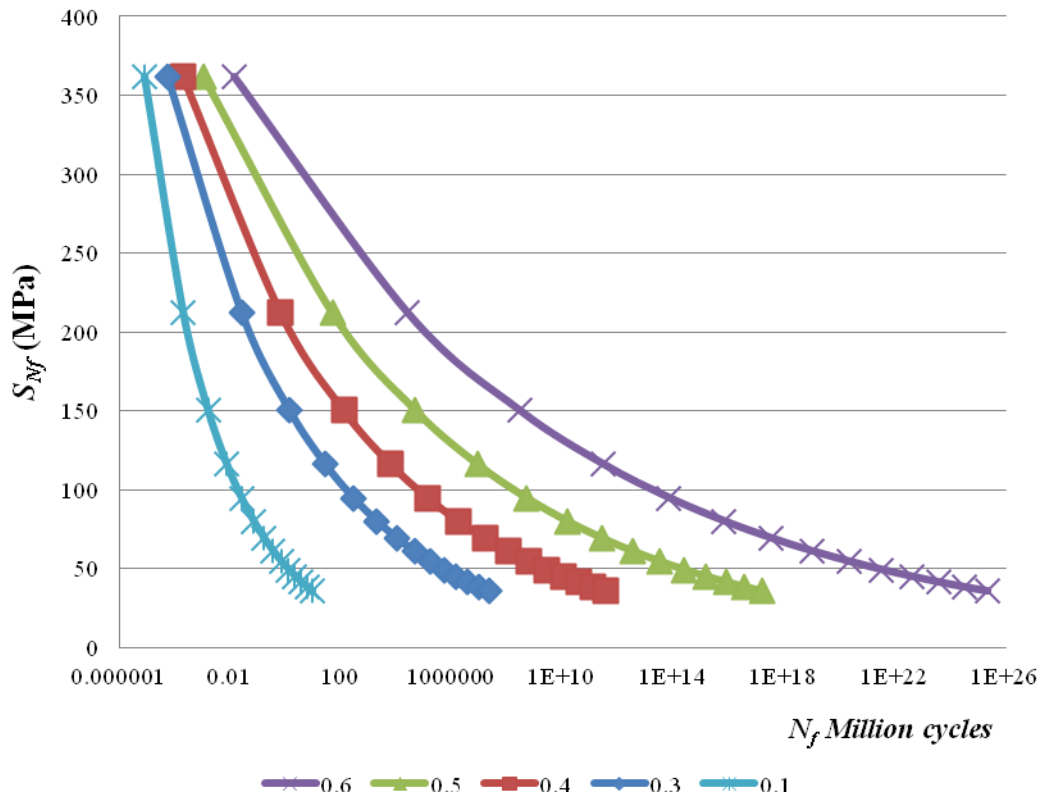


Figure 4.7: Effect of using different  $S_f$  coefficient on fatigue cycles.

From Figure 4.7, it can be seen that materials or composite system with lower value of  $S_f$  coefficient will tend to fail at much lower fatigue cycles. From this analysis, value of 0.1 is chosen to be this composite system parameter due to the fact that adhesively bonded composite system is much weaker than solid metals.

$$\begin{aligned}
 S_f &= x(514\text{MPa}) \\
 &= 0.1(514\text{MPa}) \\
 &= 51.4 \text{ MPa}
 \end{aligned}$$

Assuming no surface finish, the value of  $S_f$  is taken as it is.

Hence;

$$\begin{aligned}
 B &= (1/6)\log (S_f/S_u) \\
 &= (1/6)\log (51.4/514)
 \end{aligned}$$

$$= -0.167$$

Apart from that, it can be noted from Eq. 1 that alternating stress or loading range plays a vital role in determining the number of fatigue cycles. Using all the parameter values, the fatigue loading program is developed using trial and error approach. This is to ensure every loading range is considered to enable suitable selection of loading range at the end of the analysis. The result analysis is shown in Figure 4.8.

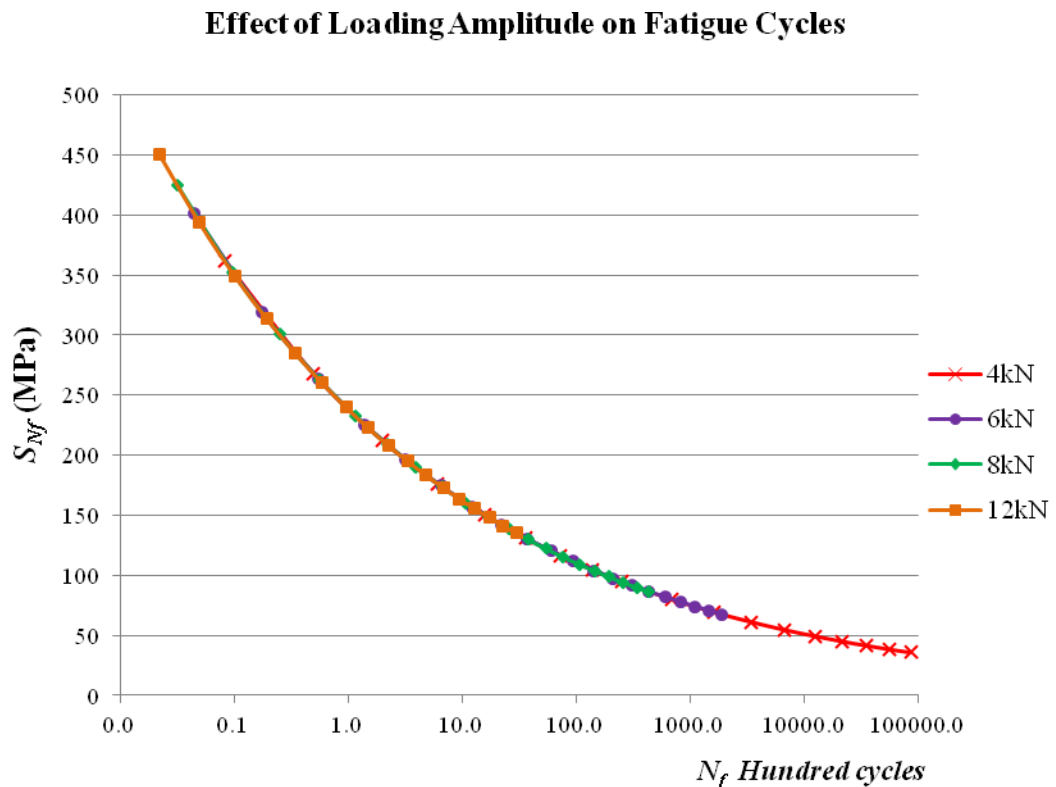


Figure 4.8: Effect of using different loading amplitude on number of cycles.

Figure 4.8 on the other hand shows that using higher amplitude of stress or loading range (12kN) will result in much lower fatigue cycles to cause the failure. However, the failure curve falls only in higher fatigue strength range, 125 MPa to 450 MPa. To achieve a well defined S-N curve that covers both low and high fatigue strength region, lower stress amplitude must be used, for instance 4kN as shown in Figure 4.8.

From these two parameters;  $S_f$  coefficient and loading range, fatigue loading program for this composite system is drawn up. Selecting suitable loading range to produce a sound S-N curve is made to ensure the experiment can be done within the time frame. The loading range for this experiment is determined to be as in Table 4.1.

Table 4.1: Fatigue loading program for CFRP plated steel member.

Loading Range (kN)		$S_{min}$ (MPa)	$S_{max}$ (MPa)	$S_a$ (MPa)	$S_m$ (MPa)	$S_{Nf}$ (MPa)	$N_f$ (Cycles)
18	30	300.00	500.00	100.000	400.000	450.877	2
20	28	333.33	466.67	66.667	400.000	300.585	25
18	24	300.00	400.00	50.000	350.000	156.707	1228
12	16	200.00	266.67	33.333	233.333	61.045	347369

Using the data in Table 4.1, the S-N curve is plotted accordingly as shown in Figure 4.9.

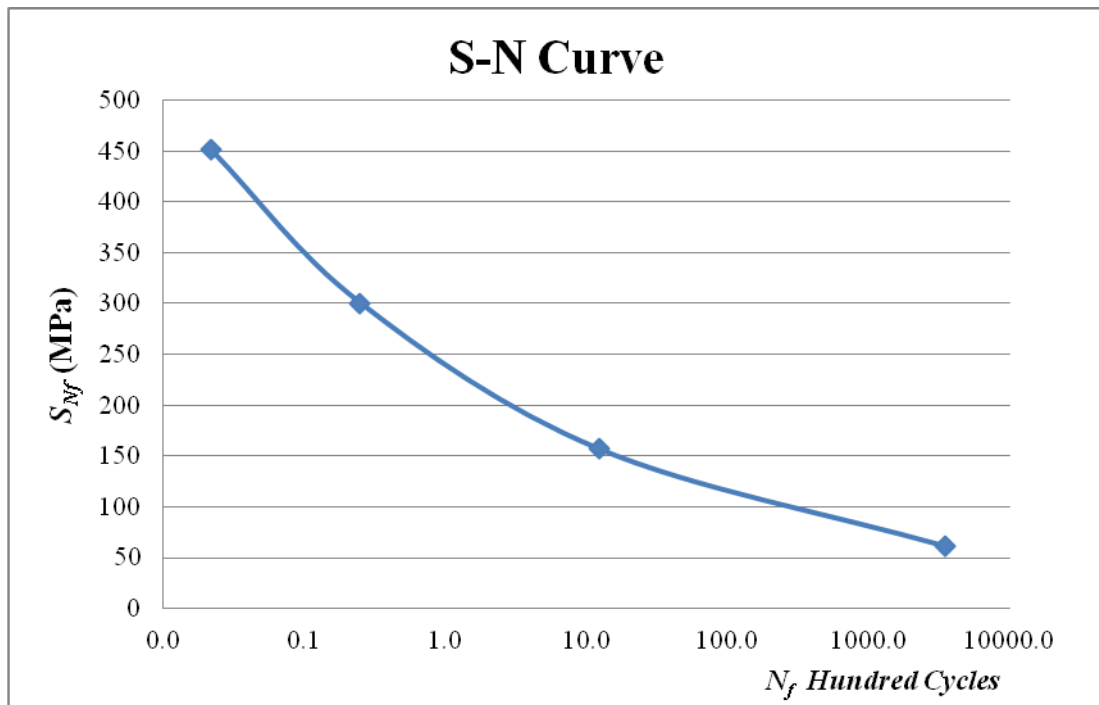


Figure 4.9: S-N curve for the proposed experimental program.

The analysis is important such that it provides the groundwork for this experiment since no experimental program is established to test the bond-slip relationship of CFRP plated steel member when subjected to fatigue loading. Also, it helps to predict the number of cycles required to cause failure in this composite system. By doing this, the experiment can be accomplished within the stipulated time frame and any deviation can be investigated and further reasoned.



## CHAPTER 5

### CONCLUSION AND RECOMMENDATION

The use of CFRP in steel strengthening offers great advantages; fatigue life improvement, fatigue crack arrest and increase in additional load carrying capacity. Many researchers have been carried out to study in detail how this system works and behave with respect to its application in the industry. These include the bond behavior, effective bond length, failure modes and bond-slip relationship under monotonic loading. Nevertheless, less attention has been given to the area of quantifying the bond-slip relationship of CFRP steel system under fatigue loading.

Hence, this research has presented a groundwork that can be used as the basis for the establishment of bond-slip relationship of this composite system under fatigue loading. Results from the testing have been presented and discussed to fully understand the behavior of the CFRP plated steel member. Hence, following conclusion can be drawn up from this research:

1. Shear stress distribution is likely to be at the same level along the bonded length. However, higher shear stress is to be expected near the loaded end due to local bending.
2. The fatigue life can be predicted using stress-life approach and is very much depending on the stress amplitude applied. Higher stress amplitude will cause the specimen to fail at lower fatigue cycles.

From the research, suitable testing regime and program can be properly chosen to ensure the development of a good bond-slip relationship. It is hoped that this research can help to further explore the potential of CFRP in steel structure retrofitting subjected to fatigue loading; steel bridges, jetty and platforms. Also, from this research, the CFRP to steel system behavior could be predicted hence allowing for development of design standards for fatigue conditions apart from filling in the gap where bond-slip relationship under fatigue loading is scarcely explored.

Further research can be done to study in detail the effective bond length under fatigue loading conditions in which has not been given attention. Having the system designed up to the optimal solution will reduce cost of structural retrofitting in the future.

## REFERENCES

- [1] Miller, T. C., Chajes, M. J., Mertz, D. R., & Hastings, J. N. (2001). Strengthening of steel bridge girder using CFRP plates. *Journal of Bridge Engineering*, 6(6), 514-522.
- [2] Wu, C., Zhao, X. L., Duan, W. H., & Al-Mahaidi, R. (2012). Bond characteristics between ultra high modulus CFRP laminates and steel. *Thin-Walled Structures*, 51, 147-157.
- [3] Yu, T., Fernando, D., Teng, J. G., & Zhao, X. L. (2012). Experimental Study on CFRP-to-steel bonded interfaces. *Composites: Part B*, pp. 2279-2289.
- [4] Xia, S. H., & Teng, J. G. (2005). Behavior of FRP-to-steel bonded joints. *International Symposium on Bond Behavior of FRP in Structures* (pp. 411-418). International Institute for FRP in Construction.
- [5] Zubaidy, H. A., Al-Mahaidi, R., & Zhao, X. L. (2012). Experimental investigation of bond characteristics between CFRP fabrics and steel plate joints under impact tensile loads. *Composite Structures*, 94, 510-518.
- [6] Bocciarelli, M., Colombi, P., Fava, G., & Poggi, C. (2009). Fatigue performance of tensile steel members strengthened with CFRP plates. *Composite Structures*, 87(4), pp. 334-343.
- [7] Zhao, X. L., & Zhang, L. (2007). State-of-the-art review on FRP strengthened steel structures. *Engineering Structures*, 29(8), pp. 1808-1823.
- [8] Boardman, B. (1990). Fatigue Resistance of Steel. In ASM, *ASM Handbook* (Vol. 1, pp. 673-688). ASM International. Retrieved from ASM Handbook Online.
- [9] Campbell, F. (2008). Chapter 14: Fatigue. In F. C. Campbell, *Elements of Metallurgy and Engineering Alloys* (pp. 243-264). United States of America: ASM International.
- [10] Kelly, S. M. (1997). *Virginia Tech Materials Science and Engineering*. Retrieved from Fatigue: [http://www.sv.vt.edu/classes/MSE2094\\_NoteBook/97ClassProj/anal/kelly/fatigue.html](http://www.sv.vt.edu/classes/MSE2094_NoteBook/97ClassProj/anal/kelly/fatigue.html)
- [11] Jackson, N., & Dhir, R. K. (1996). Fatigue of Metals. In N. Jackson, & R. K. Dhir, *Civil Engineering Materials* (pp. 49-51). New York: PALGRAVE.

- [12] Kumar, S. R., & Kumar, A. R. (2009). Fatigue of Steel Structure. In S. R. Kumar, & A. R. Kumar, *Design of Steel Structure*.
- [13] Hibbeler, R. C. (2008). Failure of Materials due to Creep and Fatigue. In R. C. Hibbeler, *Mechanics of Materials* (pp. 114-115). Singapore: Prentice Hall.
- [14] Nicolae, T., Gabriel, O., Dorina, I., Ioana, E., Vlad, M., & Catalin, B. (2008). *Fibre Reinforced Polymer Composites as Internal and External Reinforcement for Building Elements*.
- [15] Teng, J. G., Chen, J. F., Smith, S. T., & Lam, L. (2002). *FRP-Strengthened RC Structures*. UK: John Wiley and Sons Ltd.
- [16] Hollaway, L. C., & Cadei, J. (2003). Progress in the technique of upgrading metallic structures with advanced polymer composites. *Progress in Structural Engineering and Materials*, 5(2), p. 131.
- [17] Liu, H., Al-Mahaidi, R., & Zhao, X. L. (2009). Experimental study of fatigue crack growth behavior in adhesively reinforced steel structures. *Composite Structures*, 90, 12-20.
- [18] Colombi, P., Bassetti, A., & Nussbaumer, A. (2003). Delamination effects on cracked steel members reinforced by prestressed composite patch. *Theoretical and Applied Fracture Mechanics*, 39(1), 61-71.
- [19] Nozaka, K., Shield, C. K., & Hajjar, J. F. (2005). Effective bond length of carbon-fiber reinforced polymer strips bonded to fatigued steel bridge I-girders. *Journal of Bridge Engineering*, 10(2), 195-205.
- [20] Colombi, P., & Poggi, C. (2006). Strengthening of tensile steel members and bolted joints using adhesively bonded CFRP plates. *Construction and Building Materials*, 20(1-2), pp. 22-33.
- [21] Al-Emrani, M., Linghoff, D., & Kliger, R. (2005). Bonding strength and fracture mechanisms in composite steel-CFR elements. *International Symposium on Bond Behavior of FRP in Structures*, (pp. 433-441).
- [22] Fawzia, S., Zhao, X. L., Al-Mahaidi, R., & Rizkalla, S. (2005). Bond characteristics between CFRP and steel plates in double strap joints. *Advance in Steel Construction - an International Journal*, 1(2), 17-28.
- [23] Schnerch, D., Stanford, L., Summer, E., & Rizkalla, S. (2004). Strengthening steel structures and bridges with high modulus carbon fibre reinforced polymers: Resin selection and scaled monopole behavior. *Transportation Research Record*(1892), pp. 237-245.

- [24] Fawzia, S., Al-Mahaidi, R., Zhao, X. L., & Rizkalla, S. (2005). Strengthening of circular hollow tubular section using CFRP sheets. *Construction and Building Materials*, 21(4), 839-845.
- [25] Jiao, H., & Zhao, X. L. (2004). CFRP strengthened butt-welded very high strength (VHS) circular steel tubes. *Thin Walled Structures*, 7, pp. 963-978.
- [26] El Damatty, A. A., & Abushagur, M. (2003). Testing and Modelling of Shear and Peel Behavior for Bonded Steel/FRP Connections. *Thin Walled Structures*, 41(11), pp. 987-1003.
- [27] Wu, C., Zhao, X. L., Chiu, W. K., Al-Mahaidi, R., & Duan, W. H. (2013). Effect of fatigue loading on the bond behavior between UHM CFRP plates and steel plates. *Composites: Part B*.
- [28] Liu, H. B., Zhao, X. L., & Al-Mahaidi, R. (2005). The effect of fatigue loading on bond strength of CFRP bonded steel plate joints. *International Symposium on Bond Behavior of FRP in structures*. Hong Kong.
- [29] Bassetti, A., Nussbaumer, A., & Hirt, M. A. (2000). Crack repair and fatigue life extension of riveted bridge members using composite materials. *Proceedings of Bridge Engineering Conference* (pp. 227-238). Egypt: The Egyptian Society of Engineers.
- [30] Tavakkolizadeh, M., & Saadatmanesh, H. (2003). Fatigue strength of steel girders strengthened with carbon fibre reinforced polymer patch. *Journal of Structural Engineering*, 129(2), 186-196.
- [31] Schnerch, D., Dawood, M., Rizkalla, S., & Summer, E. (2007). Proposed design guidelines for strengthening of steel bridges with FRP materials. *Construction Building Material*, 21, 1001-1010.
- [32] Jiao, H., Mashiri, F., & Zhao, X. L. (2012). A comparative study on fatigue behavior of steel beams retrofitted with welding, pultruded CFRP plates and wet layup CFRP sheets. *Thin-Walled Structures*, 59, 144-152.
- [33] Yu, Q. Q., Chen, T., Gu, X. L., Zhao, X. L., & Xiao, Z. G. (2013). Fatigue behavior of CFRP strengthened steel plates with different degrees of damage. *Thin-Walled Structures*, 69, 10-17.
- [34] Matta, F., Karbhari, V. M., & Vitaliani, R. (2005). Tensile Response of Steel/CFRP Adhesive Bonds for the Rehabilitation of Civil Structures. *Structural Engineering and Mechanics*, 20(5), 589-608.

- [35] Colombi, P., & Fava, G. (2012). Fatigue behavior of tensile steel/CFRP joints. *Composite Structures*, 94, 2407-2417.
- [36] Deng, J., & Lee, M. M. (2007). Fatigue performance of metallic beam strengthened with a bonded CFRP plate. *Composite Structures*, 78, 222-231.
- [37] Cadei, J. M., Stratford, T. J., Hollaway, L. C., & Duckett, W. G. (2004). CIRIA C595 - Strengthening metallic structures using externally bonded fibre-reinforced polymers. *Advanced Composite Materials in Bridges and Structures (ACMBS-IV)*.
- [38] Kim, Y. J., & Harries, K. A. (2011). Fatigue behavior of damaged steel beams repaired with CFRP strips. *Engineering Structures*, 33, 1491-1502.
- [39] Imanaka, M., Nakayama, H., Morikawa, K., & Nakamura, M. (1995). Evaluation of fatigue life of adhesively bonded CFRP pipe/steel rod joints. *Composite Structures*, 31, 235-241.
- [40] Anyfantis, K. N., & Tsouvalis, N. G. (2013). Loading and fracture response of CFRP-to-steel adhesively bonded joints with thick adherents – Part I: Experiments. *Composite structures*, 850-857.
- [41] Fawzia, S., Al-Mahaidi, R., & Zhao, X. L. (2006). Experimental and finite element analysis of a double strap joint between steel plates and normal modulus CFRP. *Composite Structures*, 75, 156-162.
- [42] Majid, M. A. (2012). Factors effect on the effective length in a double strap joint between steel plates and CFRP. *International Journal of Advances in Applied Sciences (IJAAS)*, 1(1), 11-18.
- [43] Fawzia, S., & Karim, M. A. (2011). Investigation into the Bond between CFRP and Steel Plates . *International Journal of Aerospace and Mechanical Engineering*, 5(1), 13-17.
- [44] Akbar, I., Oehlers, D., & Sadakkathulla, M. A. (2013). The Effect of Steel Yielding on CFRP Plated Steel Member by Partial Interaction Theory. *Jurnal Teknologi*, 61(3), 31-39.
- [45] Dehghani, E., Daneshjoo, F., Aghakouchak, A. A., & Khaji, N. (2012). A new bond-slip model for adhesive in CFRP-steel composite systems. *Engineering Structures*, 34, 447-454.
- [46] Stephens, R. I., Fatemi, A., Stephens, R. R., & Fuchs, H. O. (2001). S-N Curve Representation and Approximations. In *Metal Fatigue in Engineering* (pp. 83-88). Canada: John Wiley & Sons, Inc.